Experimental thermocline deepening alters vertical distribution and community structure of phytoplankton in a four-year whole-reservoir manipulation

Mary Lofton[1], Dexter W Howard[1], Ryan P Mcclure[1], Heather L Wander[1], Whitney M Woelmer[1], Alexandria G Hounshell[1], Abigail S L Lewis[1], and Cayelan C Carey[1]

[1]Virginia Tech

November 24, 2022

Abstract

1. Freshwater phytoplankton communities are currently experiencing multiple global change stressors, including increasing frequency and intensity of storms. An important mechanism by which storms affect lake and reservoir phytoplankton is by altering the water column's thermal structure (e.g., changes to thermocline depth). However, little is known about the effects of intermittent thermocline deepening on phytoplankton community vertical distribution and composition or the consistency of phytoplankton responses to varying frequency of these disturbances over multiple years. 2. We conducted whole-ecosystem thermocline deepening manipulations in a small reservoir. We used an epilimnetic mixing system to experimentally deepen the thermocline in two summers, simulating potential responses to storms, and did not manipulate thermocline depth in two succeeding summers. We collected weekly depth profiles of water temperature, light, nutrients, and phytoplankton biomass as well as discrete samples to assess phytoplankton community composition. We then used time-series analysis and multivariate ordination to assess the effects of intermittent thermocline deepening due to both our experimental manipulations and naturally-occurring storms on phytoplankton community structure. 3. We observed inter-annual and intra-annual variability in phytoplankton community response to thermocline deepening. We found that peak phytoplankton biomass was significantly deeper in years with a higher frequency of thermocline deepening events (i.e., years with both manipulations and natural storms) due to weaker thermal stratification and deeper depth distributions of soluble reactive phosphorus. Furthermore, we found that the depth of peak phytoplankton biomass was linked to phytoplankton community composition, with certain taxa being associated with deep or shallow biomass peaks, often according to functional traits such as optimal growth temperature, mixotrophy, and low-light tolerance. 4. Our results demonstrate that abrupt thermocline deepening due to water column mixing affects both phytoplankton depth distribution and community structure via alteration of physical and chemical gradients. In addition, our work supports previous research that phytoplankton depth distribution and community composition interact at inter-annual and intra-annual timescales. 5. Variability in the inter-annual and intra-annual responses of phytoplankton to abrupt thermocline deepening indicates that antecedent conditions and the seasonal timing of surface water mixing may mediate these responses. Our findings emphasize that phytoplankton depth distributions are sensitive to global change stressors and effects on depth distributions should be taken into account when predicting phytoplankton responses to increased storms under global change.

Hosted file

`supplement.docx` available at https://authorea.com/users/540012/articles/604709-experimental-thermocline-deepening-alters-vertical-distribution-and-community-structure-of-phytoplankton-in-a-four-year-whole-reservoir-manipulation

Hosted file

essoar.10511995.1.docx available at https://authorea.com/users/540012/articles/604709-experimental-thermocline-deepening-alters-vertical-distribution-and-community-structure-of-phytoplankton-in-a-four-year-whole-reservoir-manipulation

Running head: Thermocline deepening affects phytoplankton

Experimental thermocline deepening alters vertical distribution and community structure of phytoplankton in a four-year whole-reservoir manipulation

Mary E. Lofton[1†], Dexter W. Howard[1], Ryan P. McClure[1], Heather L. Wander[1], Whitney M. Woelmer[1], Alexandria G. Hounshell[1a], Abigail S.L. Lewis[1], Cayelan C. Carey[1]

[1]Department of Biological Sciences, Virginia Tech, Blacksburg, VA, USA

[†]Corresponding author. 926 W. Campus Dr., Blacksburg, VA, 24060. melofton@vt.edu.

Submitted as a Research Article to *Freshwater Biology*

The authors declare no conflicts of interest.

Keywords: epilimnetic mixing, functional traits, global change, storm, whole-ecosystem experiment

[a] Present affiliation: National Centers for Coastal Ocean Science, National Ocean Service, National Oceanic and Atmospheric Administration, Silver Spring, Maryland, USA

Abstract

1. Freshwater phytoplankton communities are currently experiencing multiple global change stressors, including increasing frequency and intensity of storms. An important mechanism by which storms affect lake and reservoir phytoplankton is by altering the water column's thermal structure (e.g., changes to thermocline depth). However, little is known about the effects of intermittent thermocline deepening on phytoplankton community vertical distribution and composition or the consistency of phytoplankton responses to varying frequency of these disturbances over multiple years.
2. We conducted whole-ecosystem thermocline deepening manipulations in a small reservoir. We used an epilimnetic mixing system to experimentally deepen the thermocline in two summers, simulating potential responses to storms, and did not manipulate thermocline depth in two succeeding summers. We collected weekly depth profiles of water temperature, light, nutrients, and phytoplankton biomass as well as discrete samples to assess phytoplankton community composition. We then used time-series analysis and multivariate ordination to assess the effects of intermittent thermocline deepening due to both our experimental manipulations and naturally-occurring storms on phytoplankton community structure.
3. We observed inter-annual and intra-annual variability in phytoplankton community response to thermocline deepening. We found that peak phytoplankton biomass was significantly deeper in years with a higher frequency of thermocline deepening events (i.e., years with both manipulations and natural storms) due to weaker thermal stratification and deeper depth distributions of soluble reactive phosphorus. Furthermore,

we found that the depth of peak phytoplankton biomass was linked to phytoplankton community composition, with certain taxa being associated with deep or shallow biomass peaks, often according to functional traits such as optimal growth temperature, mixotrophy, and low-light tolerance.

4. Our results demonstrate that abrupt thermocline deepening due to water column mixing affects both phytoplankton depth distribution and community structure via alteration of physical and chemical gradients. In addition, our work supports previous research that phytoplankton depth distribution and community composition interact at inter-annual and intra-annual timescales.
5. Variability in the inter-annual and intra-annual responses of phytoplankton to abrupt thermocline deepening indicates that antecedent conditions and the seasonal timing of surface water mixing may mediate these responses. Our findings emphasize that phytoplankton depth distributions are sensitive to global change stressors and effects on depth distributions should be taken into account when predicting phytoplankton responses to increased storms under global change.

Introduction

Phytoplankton in lakes and reservoirs are ecologically important organisms that are currently experiencing multiple global change stressors (Winder & Sommer, 2012). These stressors include nutrient (Smith, 2003) and sediment pollution (Donohue & Garcia Molinos, 2009), increased frequency and intensity of storms (Kirchmeier-Young & Zhang, 2020), and increased water temperatures (O'Reilly *et al.*, 2015) that result in altered thermal stratification

(Woolway *et al.*, 2019; Dokulil *et al.*, 2021). Phytoplankton responses to these global change stressors range from changes in total biomass (Ho, Michalak & Pahlevan, 2019) to altered phenology and seasonal succession (Henson *et al.*, 2018) and changes in the presence and relative abundance (Carey *et al.*, 2012; Winder & Sommer, 2012) or spatial distribution (Stockwell *et al.*, 2020) of phytoplankton taxa. Because of the fundamental role phytoplankton play in freshwater ecosystem function, changes in the composition and distribution of phytoplankton communities can alter nutrient cycling (Cottingham *et al.*, 2015), increase or decrease ecosystem productivity and dissolved oxygen levels (Diaz, 2001), and affect food quantity and quality for higher trophic levels (Danielsdottir, Brett & Arhonditsis, 2007). Global change stressors may also increase the prevalence of algal and cyanobacterial blooms (Ho & Michalak, 2020), which can have a variety of undesirable impacts including release of toxins (Chorus & Welker, 2021), unsightly surface scums, and taste and odor problems (Watson *et al.*, 2016).

One important mechanism by which global change affects freshwater phytoplankton is via alteration of thermocline depth (Gray *et al.*, 2019), which can occur either gradually due to changing air temperatures (Kraemer *et al.*, 2015; Flaim *et al.*, 2016) or abruptly due to storms (Jennings *et al.*, 2012; Klug *et al.*, 2012; Ren *et al.*, 2020; Stockwell *et al.*, 2020). Alteration of thermocline depth can affect the vertical distribution and composition of the phytoplankton community during the summer stratified period (Garneau *et al.*, 2013; Jobin & Beisner, 2014), as phytoplankton biomass in many stratified lakes and reservoirs is shown to vary across depth, with peak biomass concentration often occurring well below the surface (Hamilton, Brien & Mcbride, 2010; Cullen, 2015; Latasa *et al.*, 2017; Leach *et al.*, 2018; Lofton *et al.*, 2020). These biomass peaks form in response to vertical environmental gradients (e.g., of water temperature

and light) within the water column (Longhi & Beisner, 2009; Cullen, 2015; Albers *et al.*, 2018; Lofton *et al.*, 2020; Reinl, Sterner & Austin, 2020), and may be especially sensitive to global-change induced alteration of thermal stratification (Carey *et al.*, 2012; Winder & Sommer, 2012).

Changes in thermocline depth may affect both the depth and width of phytoplankton biomass peaks (Fig. 1; Beisner & Longhi, 2013; Jobin & Beisner, 2014; Leach *et al.*, 2018; Lofton *et al.*, 2020), as well as phytoplankton community composition (Lydersen & Andersen, 2007; Jobin & Beisner, 2014; Stockwell *et al.*, 2020). Deepening thermoclines can increase the proportion of the water column where light availability and water temperature are suitable for phytoplankton growth (Huisman *et al.*, 2004) or entrain nutrients from below the thermocline into the photic zone (Stockwell *et al.*, 2020). As a result, thermocline deepening could either lead to: 1) a deeper phytoplankton biomass peak as phytoplankton shift to access entrained nutrients (Fig. 1B; e.g., Garneau *et al.*, 2013), or 2) a wider, more diffuse peak as some phytoplankton shift their depth to maximize entrained nutrient availability while others remain at shallow depths to maximize light availability (Fig. 1C; e.g., Jobin & Beisner, 2014). Additionally, a thermocline that is shallower than the photic zone depth might favor taxa that are tolerant of high ultraviolet radiation and grow well at warm temperatures, while a deeper thermocline might favor taxa that are low-light tolerant or mixotrophic (Klausmeier & Litchman, 2001; Diehl *et al.*, 2002; Huisman *et al.*, 2004).

Gradual changes in thermocline depth due to air temperature warming and abrupt changes in thermocline depth due to storms likely evoke different phytoplankton responses at different time scales. Whole-ecosystem studies examining the response of phytoplankton to gradual thermocline deepening over multiple years, as might occur due to warming air temperatures, found that thermocline deepening affected the relative abundance of phytoplankton

taxa and phytoplankton vertical distributions (Lydersen & Andersen, 2007; Cantin *et al.*, 2011; Jobin & Beisner, 2014). Specifically, thermocline deepening increased species richness, decreased the abundance of chlorophytes and diatoms, and increased the abundance of mixotrophic dinoflagellates in an oligotrophic Norwegian lake over three years, although total phytoplankton biomass did not change (Lydersen & Andersen, 2007). Conversely, thermocline deepening led to increased chlorophyte abundance and total biomass (Cantin *et al.*, 2011) and shallower, wider biomass peaks of phytoplankton (Jobin & Beisner, 2014) in different summers during a multi-year whole-ecosystem experiment in an oligotrophic lake in Québec, Canada. These contradictory findings highlight the possibility for multiple mechanisms of thermocline deepening effects on phytoplankton community structure.

Variability in observed whole-ecosystem effects of a single abrupt thermocline deepening event on phytoplankton at daily to seasonal timescales (Rinke *et al.*, 2009; Garneau *et al.*, 2013; Wu *et al.*, 2015; Planas & Paquet, 2016; Kasprzak *et al.*, 2017) underscores the need for improved understanding of the potential cumulative effects of an increased frequency and intensity of multiple abrupt thermocline deepening events, especially at the inter-annual scale. Previous studies looking at single thermocline deepening events have observed conflicting results. Several studies which examined the effect of a single storm event on phytoplankton vertical distributions at the whole-ecosystem scale reported homogenization of biomass across the epilimnion (warm surface waters) after a storm due to internal seiches, upwelling, and surface water mixing (Rinke *et al.*, 2009; Wu *et al.*, 2015; Planas & Paquet, 2016; Kasprzak *et al.*, 2017; represented in Fig. 1C). In contrast, another study did not report homogenization but instead a deepened biomass maximum after a storm (Garneau *et al.*, 2013; represented in Fig. 1B). Finally, abrupt experimental thermocline deepening caused increases in small, silica-

containing flagellates and decreases in colonial, filamentous phytoplankton taxa but inconsistent total biomass responses during a single summer (Lofton *et al.*, 2019). These varying responses to single events highlight the pressing need to understand the *cumulative* response of phytoplankton to an increased frequency and intensity of intermittent, abrupt thermocline deepening, such as might occur due to an increasing frequency of storm events, over multiple years due to global change.

The relationship between the frequency of abrupt thermocline disturbance and phytoplankton community structure over multiple summers has important implications for the predictability of phytoplankton community response to increased storms. Some research suggests that an increased frequency and intensity of thermocline deepening disturbance could result in greater rates of change in the presence and relative abundance of phytoplankton taxa (Pannard, Bormans & Lagadeuc, 2008). Alternatively, as the frequency of thermocline deepening events increases, the phytoplankton community could shift to include more taxa that are well-adapted to mixed conditions (Winder & Sommer, 2012; Stockwell *et al.*, 2020). Examining the effects of thermocline deepening events at varying frequencies over multiple years will enhance our ability to predict phytoplankton community responses to future increases in storm frequency.

We conducted a whole-ecosystem manipulation in which we experimentally deepened the thermocline of a small, eutrophic reservoir and examined the responses of phytoplankton depth distribution and community structure over four years. Our study addressed two research questions: 1) How do phytoplankton depth distribution and community structure change in response to an increased frequency of thermocline deepening events? and 2) What are the duration and consistency of these responses at intra-annual and inter-annual scales? We performed five thermocline deepening manipulations over two summers, and then did not

manipulate the thermocline in two reference summers. We monitored phytoplankton depth distribution and community structure weekly. We also measured a suite of physicochemical variables to assess responses to changes in gradients of light, temperature, and nutrients associated with thermocline deepening on weekly to inter-annual timescales.

Methods

Study site

We conducted two summers of thermocline deepening manipulations (2016–2017), followed by two summers with no manipulations (2018–2019) in Falling Creek Reservoir (FCR), a small drinking water supply reservoir located in Vinton, VA, USA (37°18′12″ N, 79°50′14″ W; Fig. 2). FCR is owned and operated by the Western Virginia Water Authority (WVWA), has a maximum depth of 9.3 m (Fig. 2), and is thermally stratified from approximately April to October each year (Carey *et al.*, 2021c), with ice cover and inverse stratification occurring intermittently during the winter months in most years (Carey, 2021). From May to September in 2016–2019, FCR's trophic state indicated mesotrophic to eutrophic conditions (following Carlson & Simpson, 1996): mean total phosphorus (TP) across the water column was 19 ± 11 μg L^{-1} (1 S.D.), mean total nitrogen was 343 ± 242 μg L^{-1} (Carey *et al.*, 2020a), and mean Secchi depth was 2.0 ± 0.7 m (Carey *et al.*, 2020b). Over the course of the study, water residence time in FCR had a median of 174 days (Carey *et al.*, 2021b; see Text S1), and the reservoir was managed to have a constant water level.

184

185 *Thermocline deepening manipulations*

186 An engineered bubble-plume epilimnetic mixing (EM) system was deployed in FCR for
187 water quality management (Visser *et al.*, 2016). The EM is installed at a depth of 5 m and
188 extends throughout the lacustrine region of the reservoir (Fig. 2). The system comprises an
189 onshore air compressor coupled to a diffusor line of porous hose which can inject bubbles of
190 atmospheric air into the water column at rates up to 25 standard cubic feet per minute (SCFM;
191 see Lofton et al. 2019 for an in-depth description of the EM system).

192 In 2016 and 2017, we conducted a total of five discrete, short (24–72-hour)
193 manipulations in FCR to test operation of the EM in collaboration with the WVWA.
194 Manipulations occurred in late May, late June, and late July of 2016 and in late May and early
195 July of 2017 and had varied timing, intensity, and duration (Table 1) to provide the WVWA with
196 information on the effects of EM operation under a range of conditions. These short, intense
197 thermocline deepening manipulations are well-suited to simulate the abrupt changes in
198 thermocline depth that can accompany storms (e.g., Kasprzak *et al.*, 2017) and contrast with
199 previous empirical work examining phytoplankton response to thermocline deepening via
200 gradual mixing (Lydersen & Andersen, 2007; Cantin *et al.*, 2011; Jobin & Beisner, 2014). EM
201 system testing was halted after two years and so the thermocline formed in the absence of
202 manipulations during the summers of 2018 and 2019.

203

204 *Field sampling*

205 To identify naturally-occurring storm events that might result in thermocline deepening,
206 we measured wind speed (05103-L Wind Monitor, R.M. Young, Traverse City, MI, USA) and

precipitation (TE525WS-L Rain Gauge, Texas Electronics, Dallas, TX, USA) at one-minute temporal resolution throughout the study period with a meteorological station (CR3000 Micrologger, Campbell Scientific, Logan, UT, USA) deployed on the dam of FCR (Fig. 2; Carey *et al.*, 2021a).

To assess the effect of thermocline deepening on phytoplankton, we collected weekly depth profiles of phytoplankton biomass and grab samples for microscope identification of phytoplankton taxa from May to September in 2016–2019. All sampling was conducted at the deepest site of the reservoir (Fig. 2). Biomass depth profiles (~10 cm resolution) were collected using a FluoroProbe (bbe Moldaenke, Schwentinental, Germany; Catherine *et al.*, 2012; Carey *et al.*, 2021c). FluoroProbes report total biomass as the summation of biomass across four spectral groups (green algae, brown algae, cyanobacteria, and cryptophytes; Beutler *et al.*, 2002). For this study, we focused on total biomass profiles (vs. individual spectral groups) to represent the entire community's depth distribution patterns. We chose to sample phytoplankton community composition at the depth of peak phytoplankton biomass according to total biomass profiles. Depth samples were collected using a 4-L van Dorn sampler (Wildco, Yulee, FL, USA) at the depth of peak biomass estimated from FluoroProbe depth profiles. Samples were immediately preserved in opaque 250 mL high-density polyethylene (HDPE) bottles by adding ~1% Lugol's iodine by volume for subsequent microscope analysis.

We also collected a suite of physicochemical variables each week to assess the effect of thermocline deepening over the four-year study. We obtained ~0.1 m-resolution depth profiles of water temperature (Carey *et al.*, 2020b, 2021c e) and photosynthetically active radiation (Carey *et al.*, 2020b, 2021c) and measured Secchi depth (Carey *et al.*, 2020b). We also collected 1-2 m-resolution depth profiles of water chemistry, including dissolved organic carbon (DOC), nitrate

(NO_3), ammonium (NH_4), and soluble reactive phosphorus (SRP; Carey *et al.*, 2020a). Detailed field sampling methods for physicochemical variables can be found in Text S2.

Laboratory analyses

Phytoplankton grab samples were enumerated on a Nikon Eclipse Ci microscope (Nikon, Minato City, Tokyo, Japan). Before counting, samples were permanently mounted on slides following Crumpton (1987). Samples were then enumerated at 400× until at least 300 natural units (either single cells or colonies) had been counted (Acker, 2002; Brierley *et al.*, 2007). Phytoplankton were identified to genus and the first ten natural units of each genus were measured and used to calculate biovolume following Hillebrand *et al.* (1999). All phytoplankton microscopy was conducted by M.E.L.

All chemistry samples were analyzed following standard methods within six months of collection (Carey *et al.*, 2020a; Text S3). All data associated with this study are published in the Environmental Data Initiative repository (Carey *et al.*, 2020a b, 2021a, b, c, d e; Carey, 2021; Lofton *et al.*, 2021).

Calculation of phytoplankton community and distribution metrics

We calculated multiple metrics to describe both phytoplankton biomass depth distributions and community composition at the depth of maximum biomass. First, we used the fluorescence-based depth profiles to calculate the depth of maximum phytoplankton biomass, the magnitude of biomass at that depth, and width of the biomass peak (peak width) across depth (following Leach *et al.*, 2018; Lofton *et al.*, 2020). We determined the closest depth above and below the depth of maximum biomass where phytoplankton biomass concentration was less than

or equal to the median concentration across the water column. The difference between these two depths was assigned as the peak width (see Fig. S1 for a visual explanation of peak width calculation).

Second, we used phytoplankton count data to assess community composition at the depth of peak biomass. We determined genus richness and calculated the relative abundance and Shannon diversity of phytoplankton groups (diatoms, chlorophytes, chrysophytes, cryptophytes, cyanobacteria, desmids, dinoflagellates, euglenoids, raphids) at the depth of maximum biomass on each sampling day. To assess potential changes in both the relative abundance and the presence/absence of genera over time, we also calculated Bray-Curtis and Jaccard dissimilarity between samples each week within each year using the *vegdist* function of the *vegan* package (Oksanen *et al.*, 2020).

Calculation of physicochemical metrics

We analyzed field data to calculate metrics describing the temperature, light, nutrient, and carbon conditions in the reservoir following previous studies (Jobin & Beisner, 2014; Cullen, 2015; Leach *et al.*, 2018; Lofton *et al.*, 2020). Thermocline depth, Schmidt stability, and buoyancy frequency were calculated using the R package *rLakeAnalyzer* (Winslow *et al.*, 2019). In addition, we determined the water temperature at the depth of peak phytoplankton biomass and phytoplankton depth sample on each sampling day. Photic zone depth was determined from PAR depth profiles as the depth where 1% of incident surface light was available, and the coefficient of light attenuation (K_d) was calculated as the slope of the best fit line of the natural logarithm of percent surface light plotted against depth (Wetzel & Likens, 1991). We also determined the percent of surface light that was available at the depth of peak biomass and

phytoplankton depth sample on each sampling day. To characterize carbon and nutrient conditions, we determined the concentration of DOC, dissolved inorganic nitrogen (DIN, calculated as the sum of NO_3 and NH_4), and SRP at the sampling depth closest to the biomass peak and phytoplankton depth sample on each sampling day, as well as the coefficient of variation of carbon and nutrients across the photic zone. We also determined the magnitude of maximum observed carbon and nutrient concentrations across the photic zone on each sampling day, as well as the depth at which each concentration's maximum occurred.

Assessing effects of naturally-occurring intense storms

To determine whether our thermocline deepening manipulations approximated naturally-occurring storms, we calculated daily sums of precipitation and daily mean wind speed during the four-year study period to identify intense storms. Intense storms were defined as when both daily mean wind and summed precipitation were in the top 5% of all observation days (total n = 572) across the study period (following Doubek *et al.*, 2021). Following this, we identified two intense storm events during our four-year study period: one on 5 May 2016 and one on 8 June 2019. We then examined thermocline depths immediately before and after these naturally-occurring intense storm events (within ± 1 week) and compared them to changes in thermocline depth due to our manipulations.

Across the four years, manipulation summers experienced four (2016) or two (2017) thermocline deepening events (natural + experimental summed), whereas the reference summers experienced zero (2018) or one (2019) thermocline deepening events, representing a substantial difference in thermocline deepening frequency between manipulation and reference summers (Table 1).

Assessing effects of increased thermocline deepening frequency

We used Anderson-Darling tests (Razali & Wah, 2011) to assess the effects of increased thermocline deepening frequency, including both natural and experimental thermocline deepening events, on physicochemical and phytoplankton community structure metrics at the inter-annual scale. Anderson-Darling tests can be used to assess significant differences between distributions of a variable and give more weight to distribution tails or extreme values, permitting assessment of whether manipulations shifted both the mean and range of ecosystem variables (Razali & Wah, 2011). We considered a variable to be responsive to an increased frequency of thermocline deepening if variable distributions between summers with manipulations and reference summers were significantly different. All Anderson-Darling test p-values were Holm-Bonferroni corrected for multiple comparisons (Holm, 1979).

Analysis of phytoplankton depth distributions

We used autoregressive integrated moving average (ARIMA) models to assess how an increased frequency of thermocline deepening events affected phytoplankton depth distributions. ARIMA models are a well-established method for identifying the most important predictors of a response variable over time while accounting for autocorrelation (Hyndman & Athanasopoulos, 2018). We developed best-fit ARIMA models using physicochemical metrics to predict phytoplankton peak depth, peak width, and the magnitude of biomass at the peak depth over time. We fit models to the full time-series of depth distribution profiles (2016–2019) as well as to manipulation summers (2016-2017) and reference summers (2018-2019) separately, and then compared predictors of phytoplankton depth distributions between manipulation and reference summers and the full time-series. We did not fit ARIMA models to phytoplankton vertical

distribution time series for each individual summer or before and after thermocline deepening events or intense storms within a year because each summer's time series had <20 observations.

We developed a model selection algorithm based on the *auto.arima* function in the *forecast* package in R (Hyndman & Khandakar, 2008; Hyndman *et al.*, 2021). Our algorithm compared models fit by *auto.arima* using all possible combinations of predictors to a global model using all predictors and a null model using no predictors. The algorithm then selected the model with the lowest corrected Akaike Information Criterion (AICc) as well as all models within 2 units of the lowest AICc value (Burnham & Anderson, 2002). The models had a maximum of one autoregressive term (AR(1)), following results of partial autocorrelation functions (Hyndman & Athanasopoulos, 2018) calculated for each depth distribution metric (Fig. S2).

We considered the water temperature, light, and carbon and nutrient concentration metrics described above as potential predictors of phytoplankton peak depth, peak width, and the magnitude of biomass at the peak depth. We conducted pairwise Spearman correlations among all potential predictors; if two potential predictors had a pairwise Spearman's $\rho \geq 0.7$, we selected the predictor that was most strongly correlated with the corresponding response variable (Table S1). The distributions of all predictors and response variables were checked for skewness, log-transformed if appropriate, and standardized to Z-scores before fitting ARIMA models.

Analysis of phytoplankton community data

To relate phytoplankton community structure to physicochemical and phytoplankton depth distribution metrics, we conducted a non-metric multidimensional scaling analysis (NMDS) and post-hoc tests on ordination output. We used NMDS because this ordination

345 technique does not assume a multivariate normal distribution of community data and does not
346 constrain ordination results based on environmental gradients (McCune & Grace, 2002), which
347 was appropriate given the non-normal distribution of our data and our goal of assessing
348 community responses to thermocline deepening. We used the *metaMDS* function in the *vegan*
349 package to perform NMDS analyses across all summers (2016–2019) as well as for each summer
350 individually. This function provides the benefit of including several random starts of the NMDS
351 ordination process to ensure a stable result (Oksanen *et al.*, 2020). We assessed the stress of each
352 ordination result to determine the minimum number of axes needed to adequately explain
353 variability in community composition data (McCune & Grace, 2002).
354 We subsequently conducted several post-hoc analyses of our phytoplankton community
355 data and ordination output. We used analysis of similarities (ANOSIM) on NMDS ordination
356 output to assess phytoplankton community differences among summers and months, between
357 manipulation and reference summers, and before and after thermocline deepening events and
358 intense natural storm events within a summer. ANOSIM is an appropriate post-hoc test for
359 NMDS ordinations because both operate using ranked dissimilarities (McCune & Grace, 2002)
360 ANOSIM tests report an R statistic, where values approaching 0 indicate similar groups, values
361 approaching 1 indicate dissimilar groups, and values less than 0 indicate greater dissimilarity
362 within a group than among groups (McCune & Grace, 2002). We considered month of year to be
363 a proxy for change in the phytoplankton community due to seasonal succession, and so
364 conducting ANOSIM tests on both month of year and the periods before and after thermocline
365 deepening events within a summer allowed us to compare the relative importance of seasonal
366 succession and thermocline deepening manipulations at the intra-annual scale. Although an
367 intense storm occurred on 5 May 2016, no ANOSIM test was conducted for phytoplankton

communities before and after this storm event due to insufficient pre-storm data (n = 1 pre-storm sampling point).

We also examined associations between phytoplankton genera and manipulation vs. reference summers, periods before and after thermocline deepening events or intense storms within a summer, and each summer and month using indicator species analysis (*multipatt* function in the *indicspecies* package; De Cáceres, Jansen & Dell, 2020). We selected the *multipatt* method for indicator species analysis because it permits species to be significantly associated with more than one group (e.g., a genus can be associated with both July and August communities; see De Cáceres, Legendre & Moretti, 2010).

Finally, we evaluated associations between physicochemical variables, depth distribution metrics, and phytoplankton community structure ordination output using the *envfit* and *ordisurf* functions in the *vegan* package. Briefly, the *envfit* function fits linear models between vectors of environmental variables and ordination scores and determines which fits are significant, and the *ordisurf* function fits a smoothed surface of an environmental variable to ordination scores using a generalized additive model (GAM; Oksanen *et al.*, 2020).

All analyses were conducted in the R statistical environment (v. 4.0.3; R Core Team 2020). All analysis code is available on GitHub (https://github.com/melofton/FCR-phytos) and published via Zenodo (DOI: 10.5281/zenodo.5146268).

Results

Thermocline deepening manipulations were representative of intense storms

Comparison of our thermocline deepening manipulations with two naturally-occurring intense storms during the study period revealed that our manipulations reasonably approximated storm-induced thermocline deepening. A storm on 5 May 2016 deepened the thermocline from 3.1 to 4.2 m (change of 1.1 m), and a storm on 8 June 2019 led to a 0.3 m deepening of the thermocline (Table S2; Fig. S3; Fig. S4), while changes in thermocline depth due to our manipulations ranged from 0.5 to 3.1 m (Table S2; Fig. S3).

Increased frequency of thermocline deepening altered physicochemical variables

Multiple thermocline deepening manipulations in 2016 and 2017 significantly altered the summer thermal structure of FCR compared to reference summers, despite the occurrence of an intense storm in 2019 (Table 2; Fig. 3). The manipulations deepened the thermocline by over a meter on average (Fig. 3A, B; Fig. 4), as mean thermocline depth in manipulation summers was 3.9 ± 1.1 m (1 S.D.), vs. 2.8 ± 0.4 m in reference summers (adj. Anderson-Darling $p = 0.0004$). In addition to being deeper, thermocline depth was also more variable in manipulation summers (Fig. 3A, B).

Thermocline deepening decreased thermal stratification (Table 2; Fig. 3), with a mean Schmidt stability of 25.1 ± 8.4 J m^{-2} in manipulation summers vs. 36.9 ± 6.7 J m^{-2} in reference summers (adj. Anderson-Darling $p < 0.0001$; Fig. 3C, D). Buoyancy frequency was also significantly lower in manipulation summers ($6.1 \times 10^{-3} \pm 1.8 \times 10^{-3}$ s^{-1}) vs. reference summers ($9.3 \times 10^{-3} \pm 2.0 \times 10^{-3}$ s^{-1}; adj. Anderson-Darling $p < 0.0001$; Fig. 3E, F).

SRP depth distributions across the photic zone were different in manipulation and reference summers (Table 2; Fig. 3). Thermocline deepening manipulations increased the depth of maximum SRP concentration in the photic zone by over a meter, and the depth of maximum SRP was also more variable in manipulation summers (Fig. 3G, H; Fig. 4). The mean summer depth of maximum SRP concentration within the photic zone was 1.2 ± 0.7 m during reference summers and 2.4 ± 1.7 m in manipulation summers (adj. Anderson-Darling p = 0.0008). The magnitude of maximum summer SRP concentration in the photic zone ranged from 7 to 20 $\mu g\ L^{-1}$ across all summers (Fig. 4), but was not different between manipulation and reference summers (Table S3).

Several metrics of DOC in the photic zone were also different between manipulation and reference years (Table 2). However, this was primarily due to lower DOC concentrations in 2016 compared to all other years. As such, we considered evidence of a manipulation effect on DOC to be inconclusive. No other metrics of water temperature, light, nutrients, or carbon were significantly different between manipulation and reference years (Table S3).

Deeper maximum phytoplankton biomass in manipulation years

Phytoplankton depth distributions were altered by an increased frequency of thermocline deepening (Table 2; Fig. 3I, J) in support of the hypothesis presented in Fig. 1B. Peak biomass depth ranged from 0.31 – 7.25 m in 2016–2019, and the mean depth of maximum phytoplankton biomass was significantly deeper in manipulation summers (4.5 ± 1.3 m) than in reference summers (3.1 ± 1.3 m; adj. Anderson-Darling p = 0.003). Across all years, the median depth of maximum summer phytoplankton biomass was below the thermocline and above the depth of 1% available surface light (photic zone depth; Fig. 4).

Increased thermocline deepening frequency did not affect the width of the biomass peak or the magnitude of biomass at the peak biomass depth (Table S3). High-biomass events (i.e., blooms, defined as more than two standard deviations greater than the mean biomass for 2016–2019) occurred in 2017 and 2019 (Fig. S5), indicating that manipulations neither consistently caused nor prevented bloom formation.

Predictors of depth distributions differed between manipulation and reference summers

Physicochemical predictors of phytoplankton depth distributions differed between manipulation and reference summers (Table 4; Table S9). Overall, metrics of thermal stratification tended to be more important in best-fit ARIMA models for manipulation summers, while metrics characterizing the light environment tended to be more important in models fit for reference summers. Nutrient conditions were important in all summers.

The best-fit ARIMA model for peak depth across all summers and during manipulation summers included Schmidt stability, thermocline depth, and the depth of maximum SRP in the photic zone (Table 4), all of which were significantly different between manipulation and reference summers (Table 2; Fig. 3). As Schmidt stability and thermocline depth increased, peak depth decreased, and as the depth of maximum SRP in the photic zone increased, peak depth increased. In general, manipulation summers were associated with mean lower Schmidt stability, deeper thermoclines, deeper maximum SRP, and deeper peak biomass (Table 2, Fig. 3), so the unexpected inverse relationship between thermocline depth and peak depth was likely driven by a consistent intra-annual pattern of shallower peak depths in the early fall as the thermocline deepened seasonally (Fig. 3). During reference summers, K_d was the strongest predictor of peak

458 depth, with peak depth tending to be shallower when the light attenuation rate was high (Table
459 4).

460 Despite no significant response of peak width or maximum biomass at the depth of peak
461 biomass to thermocline deepening, the predictors of these two variables significantly differed
462 between manipulation and reference summers. During manipulation years, the strongest
463 predictor of peak width was buoyancy frequency. Peak width tended to decrease as buoyancy
464 frequency increased (Table 4), so that peaks were narrowest in strongly stratified conditions. In
465 reference summers, the strongest predictor of peak width was K_d. Peak width tended to decrease
466 as K_d increased, so that peaks were narrowest when light attenuation rates were high. During
467 manipulation summers, the strongest predictor of maximum biomass at the depth of peak
468 biomass was the AR(1) term, indicating strong autocorrelation. In reference summers, maximum
469 biomass was most strongly predicted by a positive relationship with water temperature at the
470 depth of biomass maximum. The relation of biomass to SRP concentration was equivocal, with
471 biomass exhibiting a positive relation with SRP concentration in manipulation summers and a
472 negative relation with SRP concentration in reference summers and across the full time series.
473 We note that estimated coefficients for SRP concentration in maximum biomass models had high
474 standard errors and did not differ greatly from zero (Table 4).

475

476 *Increased thermocline deepening affects inter-annual phytoplankton community composition*

477 Despite no significant change in maximum biomass, phytoplankton community
478 composition was significantly different between manipulation and reference summers (Table 3;
479 Fig. 5; Fig. 6). We found that phytoplankton community composition at the inter-annual scale
480 was sufficiently explained by three NMDS ordination axes. According to post-hoc analysis of

NMDS ordination output, occurrence of experimental thermocline deepening events (along with year and month of year) strongly predicted phytoplankton community structure in the first and second dimensions of the 2016–2019 NMDS ordination (Fig. 6A). Experimental thermocline deepening within a summer was also a strong predictor (along with month of year and peak depth) of phytoplankton community structure in the second and third dimensions of the NMDS output (Fig. 6B). A post-hoc ANOSIM test indicated that phytoplankton communities were significantly different between manipulation and reference summers (ANOSIM $R = 0.15$, $p = 0.0002$; Table 3). Additionally, pairwise ANOSIM comparisons of individual summers indicated that phytoplankton communities in the two manipulation summers were not different (ANOSIM $R = 0.04$, $p = 0.18$), but that all other pairwise summer comparisons were significantly different (Table S4).

Although total genera richness did not vary between manipulation and reference summers (adj. Anderson-Darling $p = 1.0$; Table S3), a post-hoc indicator species analysis revealed that seven genera were associated with reference summer conditions, three of which were desmids (*Staurastrum* and *Staurodesmus* in 2018 and *Spondylosium* in 2019). Anderson-Darling tests also indicated that desmids were more abundant in reference summers (adj. Anderson-Darling $p = 0.03$; Table 2). Other taxa associated with reference summer communities included cryptophyte taxa (*Rhodomonas*) and green algae taxa (*Oocystis, Monomastix, Selenastrum*). No taxa were significantly associated with manipulation summer communities. From 2016–2019, genus richness in phytoplankton samples from the depth of maximum biomass ranged from 7 to 18 genera, and a total of 65 genera were observed from 2016–2019 (Table S5; see Text S4 for further description of phytoplankton community structure).

Thermocline deepening affects intra-annual phytoplankton community composition

Phytoplankton communities before and after each thermocline deepening event were different in 2016, but not 2017 (Table 3). Additionally, phytoplankton communities before and after the intense naturally-occurring storm in 2019 were substantially different (Table 3; Fig. 6). We found that phytoplankton community composition at the intra-annual scale was sufficiently explained by two NMDS ordination axes for each year. Pairwise ANOSIMs of phytoplankton communities after each deepening event in 2016 indicated that phytoplankton communities after the second and third deepening events in late June and July were different from early-season (May-early June) phytoplankton communities (Text S2; Table S6; Fig. 6). Across all summers and within each summer, phytoplankton communities were substantially different from month to month (Table 3; Text S3), as expected due to seasonal succession. However, months within manipulation summers were more dissimilar (2016 R = 0.50 and 2017 R = 0.47) than months within reference summers (2018 R = 0.24 and 2019 R = 0.33), indicating higher community turnover during reference summers.

Indicator analysis revealed that several taxa were associated with post-storm and post-thermocline-deepening communities. A colonial, filamentous cyanobacterium *(Dolichospermum),* a single-celled, flagellated mixotroph *(Rhodomonas),* and a centric diatom *(Cyclotella)* were associated with post-storm communities in 2019, as well as following thermocline-deepening manipulations in 2016. Congruence between taxa associated with late summer communities and post-storm or post-thermocline-deepening communities (e.g., *Dolichospermum, Trachelomonas, Cyclotella*; Text S3) emphasizes the difficulty of disentangling the effects of thermocline deepening or intense storms from seasonal succession (Text S5; Table S7, S8).

Both across summers and within each summer, water temperature was the physicochemical variable most strongly associated with phytoplankton community composition in NMDS ordination results (Fig. 6; Fig. 7; see Text S6 for further discussion of physicochemical variables associated with phytoplankton community structure within and among summers).

Phytoplankton community structure differed between deep and shallow biomass peaks

Different peak biomass depths were associated with different phytoplankton communities at the inter-annual and intra-annual scale (Fig. 7). Aggregated across 2016–2019, median peak depth was 3.6 m, and the inter-quartile range of peak depths was 3.1 to 4.9 m. Phytoplankton communities that occurred above and below the 3.6 m median were substantially different during 2016–2019 (ANOSIM $R = 0.28$, $p = 0.0001$; Fig. 7A, B), and phytoplankton communities that were associated with deeper peaks were also associated with deepening in the first and second dimensions of the inter-annual NMDS (Fig. 6A). According to indicator species analysis, the top two dominant genera from 2016–2019 (*Cryptomonas* and *Dolichospermum*) were associated with deep and shallow peaks, respectively (Fig. 7). In addition to *Cryptomonas*, one green algae genus (*Elakatothrix*) was associated with peaks deeper than 3.6 m, while a diverse suite of genera other than *Dolichospermum*, including green algae (nanoplankton < 5 μm GALD, *Selenastrum*), dinoflagellate (*Parvodinium*), diatom (*Nitzchia*), and cryptophyte (*Rhodomonas*) taxa were associated with peaks shallower than 3.6 m. Intra-annually, phytoplankton communities also differed in biomass peaks above and below 3.6 m in 2017 and 2019 (see Text S7 for a description of intra-annual differences in phytoplankton community structure between deep and shallow peaks).

Discussion

Our four-year whole-ecosystem manipulation revealed that an increased frequency of thermocline deepening events led to deeper phytoplankton biomass peaks at the inter-annual scale, and this effect was mediated by changes in thermal stratification and the depth of maximum SRP concentration in the photic zone. Responses of phytoplankton depth distributions to increased thermocline deepening frequency were consistent across summers, and desmids were consistently associated with reference summer conditions. However, other responses of phytoplankton to experimental thermocline deepening and intense storms, such as drivers of phytoplankton community composition, the magnitude of maximum biomass, and bloom occurrence, varied at both the inter-annual and intra-annual scale. Our results indicate that antecedent conditions (*sensu* Perga *et al.*, 2018) and the seasonal timing of thermocline deepening may mediate the effect of abrupt thermocline deepening on phytoplankton community composition and distribution. Moreover, our finding that different taxa were associated with deep and shallow biomass peaks suggests that phytoplankton depth distributions and community composition are linked at both inter-annual and intra-annual scales. Below, we discuss our results in the context of predicting phytoplankton responses to the increased frequency of thermocline deepening anticipated under global change.

Question 1: How do phytoplankton depth distribution and community structure change in response to an increased frequency of thermocline deepening events?

Our findings indicate that an increased frequency of thermocline deepening events affected phytoplankton depth distributions via alteration and increased variability of both physical and chemical gradients in the water column at the inter-annual scale. Thermocline

573 deepening manipulations weakened stratification and increased variability in thermocline depth,
574 increased the depth of maximum SRP and variability of SRP depth distributions in the photic
575 zone, and deepened phytoplankton biomass peaks, supporting the hypothesis shown in Fig. 1B.
576 These results were complemented by ARIMA models indicating that decreases in stratification
577 and increases in the depth of maximum SRP mediated the deepening of phytoplankton biomass
578 peaks in manipulation years. The finding that thermal stratification drives biomass peak depth
579 aligns with previous research suggesting that storms affect phytoplankton community structure
580 via altered thermal stratification (Stockwell *et al.*, 2020). Alteration of nutrient depth
581 distributions in response to changes in thermocline depth also aligns with expectations from
582 previous work on storms (e.g., Jennings *et al.*, 2012), but to our knowledge, the effects of these
583 alterations in nutrient depth distributions on phytoplankton depth distributions at the whole-
584 ecosystem scale has not been previously reported.

585 An increased frequency of thermocline deepening events also altered the relative
586 importance of physicochemical drivers of phytoplankton depth distributions at the inter-annual
587 scale. Specifically, more frequent thermocline deepening disrupted the ability of phytoplankton
588 to respond to depth gradients of light. In reference years, light attenuation was strongly
589 associated with both shallower and narrower biomass peaks, supporting previous findings that
590 light attenuation is the most important driver of deep chlorophyll maximum depth across a broad
591 variety of lake types under stratified conditions (Leach *et al.*, 2018). However, in manipulation
592 years, the relative importance of available light as a driver of biomass peak depth and width
593 decreased, while the relative importance of thermal stratification increased. Strong thermal
594 stratification was associated with shallower, narrower peaks in FCR, similar to results from a
595 survey of phytoplankton depth distributions in 51 lakes in Québec, Canada (Lofton *et al.*, 2020).

596 The increased importance of thermal stratification as a driver of phytoplankton depth
597 distributions in manipulation years indicates that a thermally-stratified water column may be a
598 prerequisite for phytoplankton to optimize their depth distribution in response to gradients in
599 light, supporting previous research regarding the importance of thermal stratification for
600 formation of deep chlorophyll maxima (Cullen, 2015 and references therein). Finally, our finding
601 that maximum biomass was positively associated with warm temperatures at the peak biomass
602 depth in reference years and by thermal stratification in manipulation years supports previous
603 work suggesting that strong thermal stratification, in addition to warm temperatures, is needed
604 for phytoplankton blooms to occur (Carey *et al.*, 2012; Winder & Sommer, 2012).

605 Our study indicates that the depth distribution and community composition of
606 phytoplankton are related, which may be linked to phytoplankton functional traits (*sensu*
607 Litchman, Klausmeier & Schofield, 2007). Different phytoplankton taxa were associated with
608 deep and shallow biomass peaks, and some of these associations may have been driven by trait-
609 based responses to physicochemical conditions. For example, the filamentous cyanobacterium
610 *Dolichospermum* was associated with shallow peaks across years, likely because that taxon is
611 capable of both buoyancy regulation (Walsby, 1994) and nitrogen fixation (Wood *et al.*, 2010),
612 so it does not sink out of the water column and is not dependent on entrainment of nitrogen from
613 deeper water for growth. By contrast, the cryptophyte *Cryptomonas* was associated with deeper
614 peaks, possibly due to its low light tolerance (deNoyelles Jr *et al.*, 2016) and ability to
615 metabolize organic matter settling on the thermocline via mixotrophy (Mitra *et al.*, 2016).

616 In other cases, the reasons for association of certain phytoplankton taxa with deep or
617 shallow peaks were less clear. For example, *Rhodomonas* is functionally similar to *Cryptomonas*
618 (Mitra *et al.*, 2016), but was associated with shallow peaks in 2016–2019. It is possible that this

non-intuitive association of *Rhodomonas* with shallow peaks is due to interspecific interactions of phytoplankton within the biomass peak. For example, mixotrophic *Rhodomonas* might metabolize organic carbon released via leaching or decomposition of *Dolichospermum* filaments accumulated in shallow peaks (Kritzberg *et al.*, 2004; Ye *et al.*, 2015). Recent research indicates that mixotrophy likely plays an important role in lake plankton dynamics (Gonçalves Leles *et al.*, 2018; Beisner, Grossart & Gasol, 2019), and may be important for determining community composition at the phytoplankton biomass peak in FCR.

Question 2: What are the duration and consistency of phytoplankton responses to thermocline deepening at intra-annual and inter-annual scales?

We found that phytoplankton community responses to experimental thermocline deepening and intense storm events were variable at both intra-annual and inter-annual scales. Our results indicate that the antecedent conditions and seasonal timing of thermocline deepening events may be as important as their frequency in determining phytoplankton community responses, contradicting expectations from previous research that an increased frequency of thermocline deepening events would either cause increased change in phytoplankton community structure (Pannard *et al.*, 2008) or lead to alteration of phytoplankton community structure in favor of mixing-tolerant taxa (Winder & Sommer, 2012; Stockwell *et al.*, 2020).

At the inter-annual scale, phytoplankton community composition responses were inconsistent. Specifically, different environmental drivers were associated with phytoplankton community composition at the depth of peak biomass in each year, maximum biomass was not different between manipulation and reference years, and blooms occurred in both a manipulation and a reference year and their timing was not associated with either thermocline deepening

manipulations or storms. This lack of consistency in thermocline deepening responses across years suggests that the effects of abrupt thermocline deepening on phytoplankton community composition may be mediated by other factors. For example, antecedent conditions including winter ice cover or variability in seasonal catchment conditions affecting in-lake characteristics such as water residence time could influence phytoplankton responses to thermocline deepening (Chase, 2003; Perga *et al.*, 2018; Stockwell *et al.*, 2020; Thayne *et al.*, 2021).

At the intra-annual scale, variability in phytoplankton responses to thermocline deepening in 2016 and 2017 and an intense storm in 2019 indicates that both the timing and frequency of thermocline disturbance within the summer stratified period are important. Our findings indicate that disruption of established thermal stratification in summer (mid-June to mid-September) could cause greater disruption to phytoplankton communities than in late spring (May to early June) when stratification is weaker. Differences in phytoplankton community composition among 2016 mixing periods were primarily due to communities after the third mixing event in late July being substantially different from communities earlier in the summer. In addition, phytoplankton communities were substantially different before and after an intense storm in mid-June 2019. The observed stronger response of phytoplankton community composition to thermocline deepening when thermal stratification is already established supports the framework proposed by Stockwell et al. (2020), which predicts the response of phytoplankton to storm events is mediated by their functional traits. While spring and early fall plankton communities in temperate lakes might be well-adapted to mixing and changes in stratification, summer communities are likely not (de Senerpont Domis *et al.*, 2013), and so a mid-summer thermocline deepening event could lead to greater change in community structure. Alternatively, differences in phytoplankton community structure after an intense storm in 2019

665 may be due to storm effects that we could not simulate via thermocline deepening manipulations,
666 which are discussed further below.

667 The relative consistency in seasonal succession among all years, demonstrated by the fact
668 that June and September communities did not significantly vary among years, indicates that
669 intermittent, abrupt thermocline deepening does not completely disrupt seasonal succession. The
670 maintenance of seasonal succession dynamics despite our experimental manipulations and
671 intense storms signals the potential importance of multiple mechanisms, including littoral
672 propagule seed banks, overland dispersal, and top-down control by zooplankton grazing, in
673 maintaining phytoplankton seasonal succession (Sommer *et al.*, 2012; Padisák, Vasas & Borics,
674 2016; Cottingham *et al.*, 2021).

675

676 *Limitations and future opportunities*

677 While our study provides insight into the inter-annual and intra-annual responses of
678 phytoplankton communities to intermittent, abrupt thermocline deepening, some limitations must
679 be considered. There are several differences between the effects of our experimental thermocline
680 deepening manipulations and storm effects on lake ecosystems. First, we were unable to simulate
681 storm effects such as increased inflow and nutrient loading or changes in epilimnetic water
682 temperature (e.g., Klug *et al.*, 2012; Stockwell *et al.*, 2020; Doubek *et al.*, 2021). Second, FCR's
683 engineered mixing system is installed at a depth of 5 m, or approximately the middle of the water
684 column, so mixing action is initiated from the middle of the water column rather than the surface,
685 as would occur due to precipitation and wind action from a storm. However, examination of two
686 naturally-occurring intense storm events confirmed that our thermocline deepening
687 manipulations were a reasonable representation of thermocline deepening due to natural storms,

688 and that both storm-driven mixing and epilimnetic mixing manipulations caused turnover in
689 phytoplankton community composition at the depth of peak biomass at the intra-annual scale.
690 There are also limitations conferred by our sampling program and experimental design.
691 First, phytoplankton depth distributions were likely influenced by factors in addition to
692 thermocline deepening, including inter-annual differences in water residence time, precipitation,
693 and other factors contributing to natural year-to-year variability in phytoplankton communities,
694 which can be especially pronounced in reservoirs (Hayes et al. 2017). Second, our weekly field
695 sampling protocol precluded analysis of patterns of phytoplankton community dynamics at sub-
696 weekly timescales, which may be particularly important for understanding short-term
697 phytoplankton response to storms (Stockwell *et al.*, 2020). In particular, the importance of
698 microscale turbulence (Li *et al.*, 2018; Wu *et al.*, 2019) and convective processes (Bouffard &
699 Wüest, 2019) in movement of phytoplankton cells and formation of surface blooms at short
700 timescales is well-documented, though not quantified in this study. However, the fact that we
701 still observed consistent differences in phytoplankton depth distributions between manipulation
702 and reference years supports the strength of our results and approach. Third, an alternative
703 experimental design, such as alternating summers with and without experimental manipulations,
704 might have permitted more robust comparison of manipulation and reference summers.
705 However, our experimental design was limited by drinking water quality management
706 requirements, and still enabled assessment of increased thermocline deepening frequency over
707 multiple sequential summers.
708 Our findings indicate that examination of the effects of antecedent conditions and
709 seasonal timing of storms on phytoplankton responses and consideration of inter-specific
710 interactions in biomass peaks could be promising avenues for future research. Explicit

711 consideration of how precipitation, water residence time, phytoplankton propagule seed banks,
712 pre-storm thermal stratification strength, and other antecedent conditions affect phytoplankton
713 community response to abrupt thermocline deepening could enhance our understanding of future
714 phytoplankton response to increased frequency and intensity of storms (e.g., Cottingham *et al.*,
715 2021; Thayne *et al.*, 2021). In addition, our finding that some phytoplankton taxa are associated
716 with peak depths that do not align with theoretical expectations based on functional traits signals
717 that further attention may be needed on the role of complementary co-occurrence of
718 phytoplankton taxa (e.g., Posch *et al.*, 2015) in the formation of phytoplankton depth
719 distributions.
720
721 *Conclusions*
722 Our work demonstrates that an increased frequency of thermocline deepening events has
723 the potential to alter both phytoplankton depth distributions (following Fig. 1B) and community
724 structure via alteration of both physical and chemical environmental conditions at the inter-
725 annual scale. Furthermore, our findings support previous research suggesting that phytoplankton
726 depth distribution and community composition are linked at both the inter-annual and intra-
727 annual scale. Finally, we show that responses of phytoplankton community composition to
728 intermittent, abrupt thermocline deepening are not consistent summer to summer or among
729 thermocline deepening events or storms within a summer, indicating that antecedent conditions
730 likely play an important role in mediating phytoplankton responses to increased frequency and
731 intensity of storms under global change. Overall, our findings emphasize that both the spatial
732 distribution and composition of freshwater phytoplankton communities are sensitive to

thermocline deepening at multiple scales, and so both distribution and composition must be considered when predicting phytoplankton responses to storms under global change.

Acknowledgements

M.E.L., R.P.M., and C.C.C. designed the whole-ecosystem manipulation field campaign, and all authors helped with collection and collation of field data. Analytical chemistry was conducted by M.E.L., D.W.H., H.L.W., and W.M.W; CTD data collection was led by R.P.M. and A.S.L; and all authors assisted with publication of field datasets. The field sampling program was coordinated by M.E.L., R.P.M., A.G.H., and C.C.C. M.E.L. conducted all statistical analyses and drafted the manuscript with C.C.C., D.W.H., and R.P.M. All authors read and approved the final version of the manuscript. We thank the Western Virginia Water Authority for access to field sites, Barbara Niederlehner for assistance with analytical chemistry, and Kylie Campbell, Niall Goard, Miles Goodall, Charlotte Harrell, James Maze, Beatrice Scott, Jacob Wynne, Shengyang Chen, Jon Doubek, Kait Farrell, Katie Krueger, and Nicole Ward for help with field work. We also thank Bryan Brown, Erin Hotchkiss, Madeline Schreiber, and members of the Virginia Tech Reservoir Group and Global Change Center for helpful feedback, as well as Beatrix Beisner and Taylor Leach for valuable discussions on phytoplankton vertical distributions. Funding was provided by NSF grants CNS-1737424, DEB-1753639, DBI-1933016, DBI-1933102, and DGE-1651272, the Western Virginia Water Authority, the Global Change Center at Virginia Tech, the Virginia Tech College of Science Roundtable Make-A-Difference Scholarship, and the Virginia Water Resources Research Center.

Data availability statement

All data associated with this study are published in the Environmental Data Initiative repository and are cited in the text (Carey *et al.*, 2020a b, 2021a b c d e; Carey, 2021; Lofton *et al.* 2021). All analysis code is available on GitHub (https://github.com/melofton/FCR-phytos) and published via Zenodo (DOI: 10.5281/zenodo.5146268).

References

Acker F. (2002). Protocol P-13-52 Analysis of USGS NAWQA Program Phytoplankton Samples. In: *Protocols for the analysis of algal samples collected as part of the U.S. Geological Survey National Water-Quality Assessment Program*. (Eds D.F. Charles, C. Knowles & R.S. Davis), pp. 87–96. The Academy of Natural Sciences: Patrick Center for Environmental Research–Phycology Section, Philadelphia, PA, USA.

Albers S., Winslow L., Collinge D., Read J., Leach T. & Zwart J. (2018). rLakeAnalyzer: Lake physics tools.

Beisner B.E., Grossart H.P. & Gasol J.M. (2019). A guide to methods for estimating phago-mixotrophy in nanophytoplankton. *Journal of Plankton Research* **41**, 77–89. https://doi.org/10.1093/plankt/fbz008

Beisner B.E. & Longhi M.L. (2013). Spatial overlap in lake phytoplankton: Relations with environmental factors and consequences for diversity. *Limnology and Oceanography* **58**, 1419–1430. https://doi.org/10.4319/lo.2013.58.4.1419

Beutler M., Wiltshire K.H., Meyer B., Moldaenke C., Lüring C., Meyerhöfer M., *et al.* (2002). A fluorometric method for the differentiation of algal populations in vivo and in situ.

Photosynthesis Research **72**, 39–53. https://doi.org/10.1023/A:1016026607048

Bouffard D. & Wüest A. (2019). Convection in Lakes. *Annual Review of Fluid Mechanics* **51**, 189–215. https://doi.org/10.1146/annurev-fluid-010518-040506

Brierley B., Carvalho L., Davies S. & Krokowski J. (2007). *Guidance on the quantitative analysis of phytoplankton in Freshwater Samples*. European Water Framework Directive.

Burnham K.P. & Anderson D.R. (2002). Model selection and multimodel inference: a practical information-theoretic approach

De Cáceres M., Jansen F. & Dell N. (2020). Package 'indicspecies' v 1.7.9: Relationship Between Species and Groups of Sites. https://doi.org/10.1890/08-1823.1

De Cáceres M., Legendre P. & Moretti M. (2010). Improving indicator species analysis by combining groups of sites. *Oikos* **119**, 1674–1684. https://doi.org/10.1111/j.1600-0706.2010.18334.x

Cantin A., Beisner B.E., Gunn J.M., Prairie Y.T. & Winter J.G. (2011). Effects of thermocline deepening on lake plankton communities. *Canadian Journal of Fisheries and Aquatic Sciences* **68**, 260–276. https://doi.org/10.1139/F10-138

Carey C.C. (2021). Ice cover data for Falling Creek Reservoir, Vinton, Virginia, USA for 2013-2021 ver. 3. https://doi.org/10.6073/pasta/a23233527aa90638b2cd3075627c91e6

Carey C.C., Breef-Pilz A., Bookout B.J., Lofton M.E. & McClure R.P. (2021a). Time series of high-frequency meteorological data at Falling Creek Reservoir, Virginia, USA 2015-2020 ver. 5. https://doi.org/10.6073/pasta/890e4c11f4348b3ceda802732ffa48b4

Carey C.C., Hounshell A.G., Lofton M.E., Birgand F., Bookout B.J., Corrigan R.S., *et al.* (2021b). Discharge time series for the primary inflow tributary entering Falling Creek Reservoir, Vinton, Virginia, USA 2013-2020.

https://doi.org/doi:10.6073/pasta/a93f740e3cb55e3e08258520ed2a740b

Carey C.C., Ibelings B.W., Hoffmann E.P., Hamilton D.P. & Brookes J.D. (2012). Eco-physiological adaptations that favour freshwater cyanobacteria in a changing climate. *Water Research* **46**, 1394–1407. https://doi.org/10.1016/j.watres.2011.12.016

Carey C.C., Lewis A.S., McClure R.P., Gerling A.B., Chen S., Das A., *et al.* (2021c). Time series of high-frequency profiles of depth, temperature, dissolved oxygen, conductivity, specific conductivity, chlorophyll a, turbidity, pH, oxidation-reduction potential, photosynthetic active radiation, and descent rate for Beaverdam Reservoir, Ca. https://doi.org/10.6073/pasta/5448f9d415fd09e0090a46b9d4020ccc

Carey C.C., Lofton M.E., Woelmer W.M., Hamre K.D., Doubek J.P. & McClure R.P. (2021d). Time-series of high-frequency profiles of fluorescence-based phytoplankton spectral groups in Beaverdam Reservoir, Carvins Cove Reservoir, Falling Creek Reservoir, Gatewood Reservoir, and Spring Hollow Reservoir in southwestern Virginia, USA 2014-2020 ver. https://doi.org/10.6073/pasta/54d4bd2fee1e52e36e2b0f230912d2da

Carey C.C., Wander H.L., Woelmer W.M., Lofton M.E., Gerling A.B., McClure R.P., *et al.* (2020a). Water chemistry time series for Beaverdam Reservoir, Carvins Cove Reservoir, Falling Creek Reservoir, Gatewood Reservoir, and Spring Hollow Reservoir in southwestern Virginia, USA 2013-2019 ver 7. https://doi.org/10.6073/pasta/0d29704769868facec3e238e64d35557

Carey C.C., Woelmer W.M.., Lewis A.S.L., Breef-Pilz A., Howard D.W. & Bookout B.J. (2021e). Time series of high-frequency sensor data measuring water temperature, dissolved oxygen, pressure, conductivity, specific conductance, total dissolved solids, chlorophyll a, phycocyanin, and fluorescent dissolved organic matter at discrete depths in Falli.

https://doi.org/10.6073/pasta/88896f4a7208c9b7bddcf498258edf78

Carey C.C., Wynne J.H., Wander H.L., McClure R.P., Farrell K.J., Breef-Pilz A., *et al.* (2020b). Secchi depth data and discrete depth profiles of photosynthetically active radiation, temperature, dissolved oxygen, and pH for Beaverdam Reservoir, Carvins Cove Reservoir, Falling Creek Reservoir, Gatewood Reservoir, and Spring Hollow Reservoir in southw. https://doi.org/10.6073/pasta/3e9f27971e353c8a80840b5e99a67d0c

Carlson R. & Simpson J. (1996). *A Coordinator's Guide to Volunteer Lake Monitoring Methods*. North American Lake Management Society.

Catherine A., Escoffier N., Belhocine A., Nasri A.B., Hamlaoui S., Yéprémian C., *et al.* (2012). On the use of the FluoroProbe®, a phytoplankton quantification method based on fluorescence excitation spectra for large-scale surveys of lakes and reservoirs. *Water Research* **46**, 1771–1784

Chase J.M. (2003). Community assembly: When should history matter? *Oecologia* **136**, 489–498. https://doi.org/10.1007/s00442-003-1311-7

Chorus I. & Welker M. eds (2021). *Toxic Cyanobacteria in Water : A Guide to Their Public Health Consequences, Monitoring and Management*. Taylor & Francis.

Cottingham K.L., Ewing H.A., Greer M.L., Carey C.C. & Weathers K.C. (2015). Cyanobacteria as biological drivers of lake nitrogen and phosphorus cycling. *Ecosphere* **6**, 1–19. https://doi.org/10.1890/ES14-00174.1

Cottingham K.L., Weathers K.C., Ewing H.A., Greer M.L. & Carey C.C. (2021). Predicting the effects of climate change on freshwater cyanobacterial blooms requires consideration of the complete cyanobacterial life cycle. *Journal of Plankton Research* **43**, 10–19. https://doi.org/10.1093/plankt/fbaa059

Crumpton W.G. (1987). A simple and reliable method for making permanent mounts of phytoplankton for light and fluorescence microscopy. *Limnology and Oceanography* **32**, 1154–1159. https://doi.org/10.4319/lo.1987.32.5.1154

Cullen J.J. (2015). Subsurface Chlorophyll Maximum Layers: Enduring Enigma or Mystery Solved? *Annual Review of Marine Science* **7**, 207–239. https://doi.org/10.1146/annurev-marine-010213-135111

Danielsdottir M.G., Brett M.T. & Arhonditsis G.B. (2007). Phytoplankton food quality control of planktonic food web processes. *Hydrobiologia* **589**, 29–41. https://doi.org/10.1007/s10750-007-0714-6

deNoyelles Jr F., Smith V.H., Kastens J.H., Bennett L., Lomas M., Knapp C.W., *et al.* (2016). A 21-year record of vertically migrating subepilimnetic populations of Cryptomonas spp. *Inland Waters* **6**, 172–184. https://doi.org/10.5268/IW-6.2.930

Diaz R.J. (2001). Overview of hypoxia around the world. *Journal of environmental quality* **30**, 275–281. https://doi.org/10.2134/jeq2001.302275x

Diehl S., Berger S., Ptacnik R. & Wild A. (2002). Phytoplankton, Light, and Nutrients in a Gradient of Mixing Depths: Field Experiments. *Ecology* **83**, 399–411

Dokulil M.T., de Eyto E., Maberly S.C., May L., Weyhenmeyer G.A. & Woolway R.I. (2021). Increasing maximum lake surface temperature under climate change. *Climatic Change* **165**, 1–17. https://doi.org/10.1007/s10584-021-03085-1

Donohue I. & Garcia Molinos J. (2009). Impacts of increased sediment loads on the ecology of lakes. *Biological Reviews* **84**, 517–531. https://doi.org/10.1111/j.1469-185X.2009.00081.x

Doubek J.P., Anneville O., Dur G., Lewandowska A.M., Patil V.P., Rusak J.A., *et al.* (2021). The extent and variability of storm-induced temperature changes in lakes measured with

long-term and high-frequency data. *Limnology and Oceanography* **9999**, 1–14. https://doi.org/10.1002/lno.11739

Flaim G., Eccel E., Zeileis A., Toller G., Cerasino L. & Obertegger U. (2016). Effects of re-oligotrophication and climate change on lake thermal structure. *Freshwater Biology* **61**, 1802–1814. https://doi.org/10.1111/fwb.12819

Garneau M.-E., Posch T., Hitz G., Siegwart R. & Pernthaler J. (2013). Short-term displacement of Planktothrix rubescens (cyanobacteria) in a pre-alpine lake observed using an autonomous sampling platform. **58**, 1892–1906. https://doi.org/10.4319/lo.2013.58.5.1892

Gonçalves Leles S., Polimene L., Bruggeman J., Blackford J., Ciavatta S., Mitra A., *et al.* (2018). Modelling mixotrophic functional diversity and implications for ecosystem function. *Journal of Plankton Research* **40**, 627–642. https://doi.org/10.1093/plankt/fby044

Gray E., Elliott J.A., Mackay E.B., Folkard A.M., Keenan P.O. & Jones I.D. (2019). Modelling lake cyanobacterial blooms: Disentangling the climate-driven impacts of changing mixed depth and water temperature. *Freshwater Biology* **64**, 2141–2155. https://doi.org/10.1111/fwb.13402

Hamilton D.P., Brien K.R.O. & Mcbride C.G. (2010). Vertical distributions of chlorophyll in deep, warm monomictic lakes. *Aquatic Sciences* **72**, 295–307. https://doi.org/10.1007/s00027-010-0131-1

Henson S.A., Cole H.S., Hopkins J., Martin A.P. & Yool A. (2018). Detection of climate change-driven trends in phytoplankton phenology. *Global Change Biology* **24**, e101–e111. https://doi.org/10.1111/gcb.13886

Hillebrand H., Dürselen C.-D., Kirschtel D., Pollingher U. & Zohary T. (1999). Biovolume calculation for pelagic and benthic microalgae. *Journal of Phycology* **35**, 403–424.

https://doi.org/10.1046/j.1529-8817.1999.3520403.x

Ho J.C. & Michalak A.M. (2020). Exploring temperature and precipitation impacts on harmful algal blooms across continental U.S. lakes. *Limnology and Oceanography* **65**, 992–1009. https://doi.org/10.1002/lno.11365

Ho J.C., Michalak A.M. & Pahlevan N. (2019). Widespread global increase in intense lake phytoplankton blooms since the 1980s. *Nature* **574**, 667–670. https://doi.org/10.1038/s41586-019-1648-7

Holm S. (1979). A Simple Sequentially Rejective Multiple Test Procedure. *Scandinavian Journal of Statistics* **6**, 65–70

Huisman J., Sharples J., Stroom J.M., Visser P.M., Edwin W., Kardinaal A., *et al.* (2004). Changes in Turbulent Mixing Shift Competition for Light between Phytoplankton Species. *Ecology* **85**, 2960–2970

Hyndman R., Athanasopoulos G., Bergmeir C., Caceres G., Chhay L., O'Hara-Wild, M Petropoulos F., *et al.* (2021). forecast: Forecasting functions for time series and linear models

Hyndman R. & Khandakar Y. (2008). Automatic time series forecasting: the forecast package for R. *Journal of Statistical Software* **26**, 1–22

Hyndman R.J. & Athanasopoulos G. (2018). *Forecasting: principles and practice*, 2nd edn. Otexts, Melbourne, Australia.

Jennings E., Jones S., Arvola L., Staehr P.A., Gaiser E., Jones I.D., *et al.* (2012). Effects of weather-related episodic events in lakes: an analysis based on high-frequency data. *Freshwater Biology* **57**, 589–601. https://doi.org/10.1111/j.1365-2427.2011.02729.x

Jobin V.O. & Beisner B.E. (2014). Deep chlorophyll maxima, spatial overlap and diversity in

phytoplankton exposed to experimentally altered thermal stratification. *Journal of Plankton Research* **36**, 933–942

Kasprzak P., Shatwell T., Gessner M.O., Gonsiorczyk T., Kirillin G., Selmeczy G., *et al.* (2017). Extreme Weather Event Triggers Cascade Towards Extreme Turbidity in a Clear-water Lake. *Ecosystems*, 1–14. https://doi.org/10.1007/s10021-017-0121-4

Kirchmeier-Young M.C. & Zhang X. (2020). Human influence has intensified extreme precipitation in North America. *Proceedings of the National Academy of Sciences of the United States of America* **117**, 13308–13313. https://doi.org/10.1073/pnas.1921628117

Klausmeier C.A. & Litchman E. (2001). Algal Games : The Vertical Distribution of Phytoplankton in Poorly Mixed Water Columns. *Limnology and Oceanography* **46**, 1998–2007

Klug J.L., Richardson D.C., Ewing H.A., Hargreaves B.R., Samal N.R., Vachon D., *et al.* (2012). Ecosystem effects of a tropical cyclone on a network of lakes in northeastern North America. *Environmental Science & Technology* **46**, 11693–11701. https://doi.org/10.1021/es302063v

Kraemer B.M., Anneville O., Chandra S., Dix M., Kuusisto E., Livingstone D.M., *et al.* (2015). Morphometry and average temperature affect lake stratification responses to climate change. *Geophysical Research Letters* **42**, 4981–4988. https://doi.org/10.1002/2015GL064097

Kritzberg E.S., Cole J.J., Pace M.L., Granéli W. & Bade D.L. (2004). Autochthonous versus allochthonous carbon sources of bacteria: Results from whole-lake 13C addition experiments. *Limnology and Oceanography* **49**, 588–596. https://doi.org/10.4319/lo.2004.49.2.0588

940 Latasa M., Cabello A.M., Morán X.A.G., Massana R. & Scharek R. (2017). Distribution of
941 phytoplankton groups within the deep chlorophyll maximum. *Limnology and*
942 *Oceanography* **62**, 665–685. https://doi.org/10.1002/lno.10452
943 Leach T.H., Beisner B.E., Carey C.C., Pernica P., Rose K.C., Huot Y., *et al.* (2018). Patterns and
944 drivers of deep chlorophyll maxima structure in 100 lakes: The relative importance of light
945 and thermal stratification. *Limnology and Oceanography* **63**, 628–646.
946 https://doi.org/10.1002/lno.10656
947 Li M., Xiao M., Zhang P. & Hamilton D.P. (2018). Morphospecies-dependent disaggregation of
948 colonies of the cyanobacterium Microcystis under high turbulent mixing. *Water Research*
949 **141**, 340–348. https://doi.org/10.1016/j.watres.2018.05.017
950 Litchman E., Klausmeier C.A. & Schofield O.M. (2007). The role of functional traits and trade-
951 offs in structuring phytoplankton communities: scaling from cellular to ecosystem level.
952 *Ecology*
953 Lofton M.E., Howard D.W., McClure R.P., Wander H.L., Woelmer W.M., Hounshell A.G., *et al.*
954 (2021). Time series of phytoplankton biovolume at the depth of the vertical chlorophyll
955 maximum in Falling Creek Reservoir, Vinton, VA, USA 2016-2019
956 Lofton M.E., Leach T.H., Beisner B.E. & Carey C.C. (2020). Relative importance of top-down
957 vs. bottom-up control of lake phytoplankton vertical distributions varies among
958 fluorescence-based spectral groups. *Limnology and Oceanography* **9999**, 1–17.
959 https://doi.org/10.1002/lno.11465
960 Lofton M.E., McClure R.P., Chen S., Little J.C. & Carey C.C. (2019). Whole-ecosystem
961 experiments reveal varying responses of phytoplankton functional groups to epilimnetic
962 mixing in a eutrophic reservoir. *Water* **11**, 1–23. https://doi.org/10.3390/w11020222

963 Longhi M.L. & Beisner B.E. (2009). Environmental factors controlling the vertical distribution
964 of phytoplankton in lakes. *Journal of Plankton Research* **31**, 1195–1207
965 Lydersen E. & Andersen T. (2007). Ecosystem effects of thermal manipulation of a whole lake ,
966 Lake Breisjøen, southern Norway (THERMOS project). *Hydrology and Earth System*
967 *Sciences* **12**, 509–522. https://doi.org/10.5194/hessd-4-3357-2007
968 McCune B. & Grace J.B. (2002). *Analysis of ecological communities*. MjM Software Design,
969 Gleneden Beach, OR SE - iv, 300 pages : illustrations ; 28 cm.
970 Mitra A., Flynn K.J., Tillmann U., Raven J.A., Caron D., Stoecker D.K., *et al.* (2016). Defining
971 Planktonic Protist Functional Groups on Mechanisms for Energy and Nutrient Acquisition :
972 Incorporation of Diverse Mixotrophic Strategies. *Annals of Anatomy* **167**, 106–120.
973 https://doi.org/10.1016/j.protis.2016.01.003
974 O'Reilly C.M., Sharma S., Gray D.K., Hampton S.E., Read J.S., Rowley R.J., *et al.* (2015).
975 Rapid and highly variable warming of lake surface waters around the globe. *Geophysical*
976 *Research Letters* **42**, 773–781. https://doi.org/10.1002/2015GL066235.Received
977 Oksanen A.J., Blanchet F.G., Friendly M., Kindt R., Legendre P., Mcglinn D., *et al.* (2020).
978 Package ' vegan ' v. 2.5-7: Community Ecology Package
979 Padisák J., Vasas G. & Borics G. (2016). Phycogeography of freshwater phytoplankton:
980 Traditional knowledge and new molecular tools. *Hydrobiologia* **764**, 3–27.
981 https://doi.org/10.1007/s10750-015-2259-4
982 Pannard A., Bormans M. & Lagadeuc Y. (2008). Phytoplankton species turnover controlled by
983 physical forcing at different time scales. *Canadian Journal of Fisheries and Aquatic*
984 *Sciences* **65**, 47–60. https://doi.org/10.1139/F07-149
985 Perga M.E., Bouffard D., Bruel R., Rodriguez L. & Guénand Y. (2018). Storm impacts on alpine

lakes: Antecedent weather conditions matter more than the event intensity. *Global Change Biology* **24**, 5004–5016. https://doi.org/10.1111/gcb.14384

Planas D. & Paquet S. (2016). Importance of climate change-physical forcing on the increase of cyanobacterial blooms in a small, stratified lake. *Journal of Limnology* **75**, 201–214. https://doi.org/10.4081/jlimnol.2016.1371

Posch T., Eugster B., Pomati F., Pernthaler J., Pitsch G. & Eckert E.M. (2015). Network of interactions between ciliates and phytoplankton during spring. *Frontiers in Microbiology* **6**, 1–14. https://doi.org/10.3389/fmicb.2015.01289

Razali N.M. & Wah Y.B. (2011). Power comparisons of Shapiro-Wilk , Kolmogorov-Smirnov , Lilliefors and Anderson-Darling tests. **2**, 21–33

Reinl K.L., Sterner R.W. & Austin J.A. (2020). Seasonality and physical drivers of deepth chlorophyll layers in Lake Superior, with implications for a rapidly warming lake. *Journal of Great Lakes Research* **46**, 1615–1624

Ren M., Eyto E. De, Dillane M., Poole R. & Jennings E. (2020). 13 Years of Storms: An Analysis of the Effects of Storms on Lake Physics on the Atlantic Fringe of Europe. *Water* **12**. https://doi.org/10.3390/w12020318

Rinke K., Huber A.M.R., Kempke S., Eder M., Wolf T., Probst W.N., *et al.* (2009). Lake-wide distributions of temperature, phytoplankton, zooplankton, and fish in the pelagic zone of a large lake. *Limnology and Oceanography* **54**, 1306–1322

de Senerpont Domis L.N., Elser J.J., Gsell A.S., Huszar V.L.M., Ibelings B.W., Jeppesen E., *et al.* (2013). Plankton dynamics under different climatic conditions in space and time. *Freshwater Biology* **58**, 463–482. https://doi.org/10.1111/fwb.12053

Smith V.H. (2003). Eutrophication of freshwater and coastal marine ecosystems a global

problem. *Environmental Science and Pollution Research* **10**, 126–139. https://doi.org/10.1065/espr2002.12.142

Sommer U., Adrian R., De Senerpont Domis L., Elser J.J., Gaedke U., Ibelings B., *et al.* (2012). Beyond the Plankton Ecology Group (PEG) Model: Mechanisms Driving Plankton Succession. *Annual Review of Ecology, Evolution, and Systematics* **43**, 429–448. https://doi.org/10.1146/annurev-ecolsys-110411-160251

Stockwell J.D., Doubek J.P., Adrian R., Anneville O., Carey C.C., Carvalho L., *et al.* (2020). Storm impacts on phytoplankton community dynamics in lakes. *Global Change Biology* **26**, 2756–2784. https://doi.org/10.1111/gcb.15033

Thayne M.W., Kraemer B.M., Mesman J.P., Ibelings B.W. & Adrian R. (2021). Antecedent lake conditions shape resistance and resilience of a shallow lake ecosystem following extreme wind storms. *Limnol. Oceanogr.* **9999**, 1–20. https://doi.org/10.1002/lno.11859

Visser P.M., Ibelings B.W., Bormans M. & Huisman J. (2016). Artificial mixing to control cyanobacterial blooms: a review. *Aquatic Ecology* **50**, 423–441. https://doi.org/10.1007/s10452-015-9537-0

Walsby A.E. (1994). Gas Vesicles. *Microbiological reviews* **58**, 94–144. https://doi.org/10.1146/annurev.pp.26.060175.002235

Watson S., Monis P., Baker P. & Giglio S. (2016). Biochemistry and genetics of taste- and odor-producing cyanobacteria. *Harmful Algae* **54**, 112–127. https://doi.org/10.1016/j.hal.2015.11.008

Wetzel R.G. & Likens G.E. (1991). *Limnological Analyses*, 2nd edn. Springer Science & Business Media, New York, NY, USA.

Winder M. & Sommer U. (2012). Phytoplankton response to a changing climate. *Hydrobiologia*

698, 5–16. https://doi.org/10.1007/s10750-012-1149-2

Winslow L., Read J., Woolway R., Brentrup J., Leach T., Zwart J., *et al.* (2019). rLakeAnalyzer: Lake Physics Tools

Wood S.A., Prentice M.J., Smith K. & Hamilton D.P. (2010). Low dissolved inorganic nitrogen and increased heterocyte frequency: Precursors to Anabaena planktonica blooms in a temperate, eutrophic reservoir. *Journal of Plankton Research* **32**, 1315–1325. https://doi.org/10.1093/plankt/fbq048

Woolway R.I., Weyhenmeyer G.A., Schmid M., Dokulil M.T., de Eyto E., Maberly S.C., *et al.* (2019). Substantial increase in minimum lake surface temperatures under climate change. *Climatic Change* **155**, 81–94. https://doi.org/10.1007/s10584-019-02465-y

Wu T., Qin B., Brookes J.D., Shi K., Zhu G., Zhu M., *et al.* (2015). The influence of changes in wind patterns on the areal extension of surface cyanobacterial blooms in a large shallow lake in China. *Science of the Total Environment* **518**–**519**, 24–30

Wu X., Noss C., Liu L. & Lorke A. (2019). Effects of small-scale turbulence at the air-water interface on microcystis surface scum formation. *Water Research* **167**, 115091. https://doi.org/https://doi.org/10.1016/j.watres.2019.115091

Ye L., Wu X., Liu B., Yan D. & Kong F. (2015). Dynamics and sources of dissolved organic carbon during phytoplankton bloom in hypereutrophic Lake Taihu (China). *Limnologica* **54**, 5–13. https://doi.org/10.1016/j.limno.2015.05.003

Table 1: Schedule of thermocline deepening events and field sampling from 2016–2019. †SCFM = standard cubic feet per minute.

	Thermocline deepening events				Sampling season	
Year	**Date**	**Mixer operation**	**Intensity** *(SCFM †)*	**Duration** *(hrs)*	**Start date**	**End date**
2016	May 29	continuous	25	6	May 2	Sept. 20
	June 27-28	continuous	15	24		
	July 25-27	continuous	7.5-25	56		
2017	May 30	continuous	15	24	May 15	Sept. 4
	July 10-12	intermittent (8 hrs per day)	15	72		
2018	--	--	--	--	May 7	Sept. 10
2019	--	--	--	--	May 6	Sept. 11

Table 2: Results of significant Anderson-Darling (A-D) tests to determine effect of thermocline deepening on physical, chemical, and biological variables at the inter-annual scale. All p-values were Holm-Bonferroni corrected for multiple comparisons; non-significant variables are presented in Table S3. PZ = photic zone; CV = coefficient of variation; SRP = soluble reactive phosphorus; DOC = dissolved organic carbon; BV = biovolume; RA = relative abundance

Driver	Mean ± 1 S.D. in manipulation years	Mean ± 1 S.D. in reference years	adj. A-D *p*-value	Mean ± 1 S.D. in 2016	Mean ± 1 S.D. in 2017	Mean ± 1 S.D. in 2018	Mean ± 1 S.D. in 2019
Thermocline depth (m)	3.9 ± 1.1	2.8 ± 0.4	3.2×10^{-4}	4.1 ± 1.1	3.7 ± 1	2.9 ± 0.4	2.8 ± 0.4
Schmidt stability (J m^{-2})	25.1 ± 8.4	36.8 ± 6.6	2.5×10^{-5}	24.6 ± 8.7	25.8 ± 8.3	37.6 ± 6.3	36 ± 7.1
Buoyancy frequency (s^{-1})	0.006 ± 0.0018	0.0093 ± 0.0021	3.2×10^{-6}	0.0063 ± 0.0018	0.0056 ± 0.002	0.0098 ± 0.002	0.0087 ± 0.002
Depth of max. SRP in PZ (m)	2.4 ± 1.9	1.2 ± 0.7	7.0×10^{-4}	3 ± 1.9	1.8 ± 1.8	0.9 ± 0.8	1.5 ± 0.4
Mean PZ DOC (mg L^{-1})	2.6 ± 1	4 ± 1.4	1.6×10^{-4}	2.1 ± 0.7	3.2 ± 1.1	4.6 ± 1.1	3.5 ± 1.4
Max. PZ DOC (mg L^{-1})	3.2 ± 1.4	4.7 ± 1.6	8.0×10^{-4}	2.7 ± 1.4	3.7 ± 1.2	5.5 ± 1.8	4.2 ± 1.2
DOC at peak depth (mg L^{-1})	2.5 ± 1.3	3.7 ± 1.5	1.6×10^{-3}	2.2 ± 1.3	2.9 ± 1.2	4.3 ± 0.9	3.2 ± 1.8
DOC at depth sample (mg L^{-1})	2.5 ± 1.3	3.7 ± 1.4	5.9×10^{-4}	2.2 ± 1.3	2.9 ± 1.3	4.3 ± 0.9	3.3 ± 1.7
Biomass peak depth (m)	4.5 ± 1.3	3.1 ± 1.3	2.3×10^{-3}	4.7 ± 1	4.1 ± 1.6	2.9 ± 1.1	3.2 ± 1.5
BV Desmids (μm^3 mL^{-1})	13000 ± 37000	130000 ± 180000	0.02	3800 ± 11000	26000 ± 55000	220000 ± 220000	48000 ± 90000
RA Desmids	0.01 ± 0.02	0.08 ± 0.11	0.02	0 ± 0.01	0.02 ± 0.02	0.15 ± 0.12	0.03 ± 0.06

Table 3: Analysis of similarities (ANOSIM) results conducted on non-metric multidimensional scaling (NMDS) ordination output. Phytoplankton community data were assessed for differences based on grouping by year, month, two thermocline deepening indicator variables, and one peak depth indicator variable. Pairwise ANOSIM results for year, months within a year, and month of year across years are presented in Tables S3-S6. R = ANOSIM R, where values approaching 0 indicate similar groups, values approaching 1 indicate dissimilar groups, and values less than 0 indicate greater dissimilarity within a group than among groups. P = ANOSIM p-value. †indicates the inter-annual thermocline deepening regime and was coded as 0 for manipulation years and 1 for reference years; ‡indicates the intra-annual thermocline deepening regime and was coded as 0 for reference years or pre-thermocline deepening during manipulation years, 1 for after the first thermocline deepening event within a manipulation year, 2 after the second thermocline deepening event, and 3 after the third thermocline deepening event; §assigned as a 0-1 indicator variable, where 0 was shallow peaks < 3.6 m (median peak depth across 2016–2019) and 1 was deep peaks ≥ 3.6 m. ¶Although an intense storm occurred on 5 May 2016, no ANOSIM test was conducted due to insufficient pre-storm data (n = 1 pre-storm sampling point). Significant results are italicized in bold.

NMDS input data	**Year**		**Month**		**DEEP1†**		**DEEP2‡**		**Peak biomass depth§**		**Pre- and post-intense storms¶**	
	R	***P***	***R***	***P***	***R***	***P***	***R***	***P***	***R***	***P***	***R***	***P***
2016–2019	***0.20***	***1×10^{-4}***	***0.19***	***1×10^{-4}***	***0.15***	***2×10^{-4}***	0.06	0.19	***0.28***	***1×10^{-4}***	--	--
2016	--	--	***0.50***	***1×10^{-4}***	--	--	***0.30***	***9×10^{-3}***	0.03	0.32	--	--
2017	--	--	***0.47***	***1×10^{-3}***	--	--	-0.05	0.58	***0.46***	***0.01***	--	--
2018	--	--	***0.24***	***0.04***	--	--	--	--	-0.02	0.47	--	--
2019	--	--	***0.33***	***0.01***	--	--	--	--	***0.78***	***6×10^{-4}***	***0.98***	***3×10^{-4}***

Table 4: Best-fit autoregressive integrated moving average (ARIMA) models predicting depth of peak phytoplankton biomass, peak width, and the magnitude of maximum biomass across all summers (2016–2019), as well as manipulation (abbreviated as "man"; 2016-2017) and reference ("ref"; 2018-2019) summers. ARIMA models that were within 2 corrected Akaike Information Criterion (AICc) units of the best-fit models for each response variable and time period are reported in Table S9. Note that AICc values in this table cannot be compared as models were fit to different datasets. SRP = soluble reactive phosphorus; K_d = light attenuation coefficient; DIN = dissolved inorganic nitrogen; DOC = dissolved organic carbon; CV = coefficient of variation; AR(1) = an autoregressive term with a time lag of one; MA(1) = a first-order moving average term. Model order is specified as (p,d,q) where p is the order of the autoregressive term, d is the order of the integration term, and q is the order of the moving average term.

Depth distribution metric	**Years**	**ARIMA model structure**		**Predictor variables**						**AICc**	**RMSE**
		Order	**Terms**	**Thermal environment**		**Light environment**	**Chemical environment**				
			MA(1)	*Thermocline depth (m)*	*Schmidt stability ($J\ m^{-2}$)*	*K_d*	*Depth of max. SRP in photic zone (m)*	*Depth of max. DIN in photic zone (m)*	*Depth of max. DOC in photic zone (m)*		
Peak depth (m)	all	(0,1,1)	-0.90 ± 0.06	-0.42 ± 0.13	-0.62 ± 0.16	--	0.15 ± 0.11	-0.02 ± 0.12	0.03 ± 0.12	124.08	0.74
	man	(0,0,0)	--	-0.44 ± 0.18	-0.57 ± 0.18	--	0.31 ± 0.17	-0.09 ± 0.18	-0.09 ± 0.18	65.85	0.74
	ref	(0,0,0)	--	--	-0.16 ± 0.20	-0.50 ± 0.20	0.11 ± 0.19	--	0.20 ± 0.18	70.49	0.82
					Buoyancy frequency (s^{-1})	*K_d*	*CV of SRP in photic zone*	*CV of DIN in photic zone*	*CV of DOC in photic zone*		
Peak width (m)	all	(0,0,0)	--	--	-0.31 ± 0.11	-0.13 ± 0.11	--	--	-0.11 ± 0.11	191.64	0.93
	man	(0,0,0)	--	--	-0.26 ± 0.15	--	0.18 ± 0.15	--	--	102.35	0.91
	ref	(0,0,0)	--	--	-0.22 ± 0.17	-0.34 ± 0.18	--	--	-0.16 ± 0.18	95.16	0.93
			AR(1)	*Water temperature at the depth of peak biomass (^oC)*	*Buoyancy frequency (s^{-1})*	*% of surface light at depth of peak biomass*	*SRP concentration at depth of peak biomass ($\mu g\ L^{-1}$)*	*DIN concentration at depth of peak biomass ($\mu g\ L^{-1}$)*	*DOC concentration at depth of peak biomass ($mg\ L^{-1}$)*		
Maximum biomass ($\mu g\ L^{-1}$)	all	(1,0,0)	0.55 ± 0.11	0.64 ± 0.17	--	-0.42 ± 0.14	-0.09 ± 0.11	--	--	145.30	0.70
	man	(1,0,0)	0.65 ± 0.13	--	0.23 ± 0.14	-0.22 ± 0.16	0.21 ± 0.13	--	--	81.11	0.64
	ref	(0,0,0)	--	1.1 ± 0.17	--	-0.75 ± 0.15	-0.24 ± 0.15	--	--	64.09	0.67

Figure captions

Figure 1: Conceptual figure illustrating hypothesized relationships between thermocline depth and peak phytoplankton biomass in the water column. (A) In an unmanipulated scenario, phytoplankton peak biomass occurs at a depth which optimizes light, temperature, and nutrients (optimal zone). In response to storm-induced thermocline deepening, B and C present two alternative hypotheses of phytoplankton responses. In (B), thermocline deepening shifts the location of the optimal zone for phytoplankton growth downwards as phytoplankton access nutrients that are entrained across the thermocline. In (C), thermocline deepening homogenizes biomass across depth as some phytoplankton shift deeper to access entrained nutrients while others remain at shallow depths to maximize light availability, resulting in a broader optimal zone for phytoplankton. Gray dashed lines represent the thermocline.

Figure 2: A map of Falling Creek Reservoir (FCR), located in Vinton, Virginia, USA. The EM system line shows the extent of the epilimnetic mixing diffuser line within the reservoir that was used to implement the thermocline deepening manipulations.

Figure 3: Variables that were determined to be different between manipulated (2016, 2017) and reference (2018, 2019) summers according to Anderson-Darling tests. (A, B) Thermocline depth; (C, D) Schmidt stability; (E, F) Buoyancy frequency; (G, H) Depth of maximum soluble reactive phosphorus (SRP); (I, J) Depth of peak phytoplankton biomass. Manipulation summers are shown in coral/red and reference summers are shown in teal/blue. Note the reversed y-axes in panels (A, B, G, H, I, and J) so that the water surface is at the top of the y axis. Panel G is shown without lines for improved legibility due to discrete sampling depths of SRP.

Figure 4: Distributions of the photic zone depth, thermocline, depth of peak biomass, and depth of maximum dissolved organic carbon (DOC), dissolved inorganic nitrogen (DIN), and soluble reactive phosphorus (SRP) in the photic zone during reference summers (A; 2018-2019) and manipulation summers (B; 2016-2017), as well as the magnitude of phytoplankton biomass, DOC, DIN, and SRP at the depth of the maximum for each of these variables in (C) reference and (D) manipulation summers. Variables that were significantly different between manipulation and reference summers according to Anderson-Darling tests are marked with (*).The color gradients behind panels (A) and (B) are for illustrative purposes to connect the results presented here to hypotheses presented in conceptual Figure 1.

Figure 5: Time series of relative abundance of phytoplankton divisions and total biovolume for (A, B) manipulation summers and (C, D) reference summers. Thermocline deepening manipulations in 2016 and 2017 are denoted with dashed black vertical lines, and naturally-occurring intense storms in 2016 and 2019 are denoted with solid black vertical lines.

Figure 6: (A) First and second and (B) second and third axes of non-parametric multidimensional scaling (NMDS) ordination for phytoplankton communities across all summers (2016–2019), as well as NMDS ordination results for individual summers: (C) 2016, (D) 2017, (E) 2018, and (F) 2019. Gray and black arrows in (A) and (B) are fitted vectors of physicochemical variables plotted at a $p < 0.01$ significance level, with variables that differed in manipulation vs. reference summers in black. DEEP1 indicates the inter-annual manipulation regime, coded as 0 for reference summers and 1 for manipulation summers. DEEP2 indicates the intra-annual mixing regime, coded as 0 for reference years or pre-thermocline deepening during manipulation summers, 1 for after the first thermocline deepening event within a manipulation summer, 2 after the second thermocline deepening event, and 3 after the third thermocline

deepening event. Other vector label abbreviations: Biom = magnitude of biomass in the phytoplankton biomass peak; Mo = month; N2 = buoyancy frequency; PD = phytoplankton biomass peak depth; T = water temperature at the depth of the phytoplankton grab sample (peak biomass depth); Yr = year. The month color legend in (E) applies to all sub-plots.

Figure 7: Non-parametric multidimensional scaling (NMDS) ordinations overlain with the smooth surface plane for biomass peak depth for all summers (A,B), 2016 (C), 2017 (D), 2018 (E), and 2019 (F). Plane contours are shown for median peak depth from 2016 to 2019 (3.6 m, plotted in gray) as well as the inter-quartile range of peak depth (first quartile = 3.1 m, plotted in light gray; third quartile = 4.9 m, plotted in dark gray). Genera shown in text were associated with either shallow (<3.6 m) or deep (>3.6 m) peak depth in indicator species analysis. Genus abbreviations: Aph = *Aphanocapsa*; Ast = *Asterionella*; Chl = small green algae nanoplankton (< 5 μm greatest axial linear dimension); Cry = *Cryptomonas*; Cyc = *Cyclotella*; Dic = *Dictyosphaerium*; Dol = *Dolichospermum*; Ela = *Elaktothrix*; Eug = *Euglena*; Nit = *Nitzchia*; Par = *Parvodinium*; Rho = *Rhodomonas*; Sel = *Selenastrum*; Spo = *Spondylosium*. Black arrows in (C-F) show fitted vectors of physicochemical variables (significance level for vector plotting is $p < 0.01$). Arrows that overlap (C) are labeled with a single label for legibility. DEEP2 indicates the intra-annual mixing regime, coded as 0 for reference years or pre-thermocline deepening during manipulation summers, 1 for after the first thermocline deepening event within a manipulation summer, 2 after the second thermocline deepening event, and 3 after the third thermocline deepening event. Other vector label abbreviations: Biom = magnitude of biomass in the phytoplankton biomass peak; DOC = concentration of DOC at the depth of peak biomass; Mo = month; N2 = buoyancy frequency; PD = depth of peak biomass; SRP = concentration of SRP at the depth of peak biomass; T = water temperature at the depth of peak biomass.

Figures

Figure 1

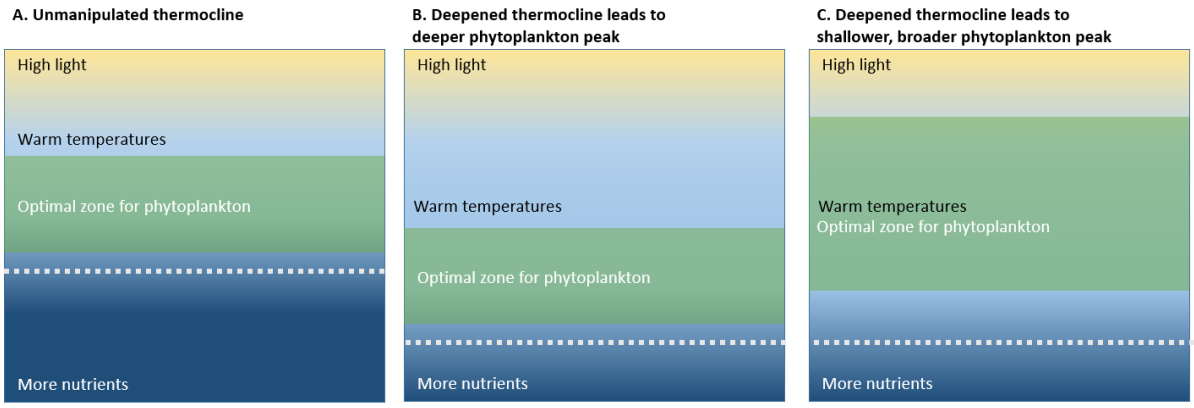

1172 Figure 2

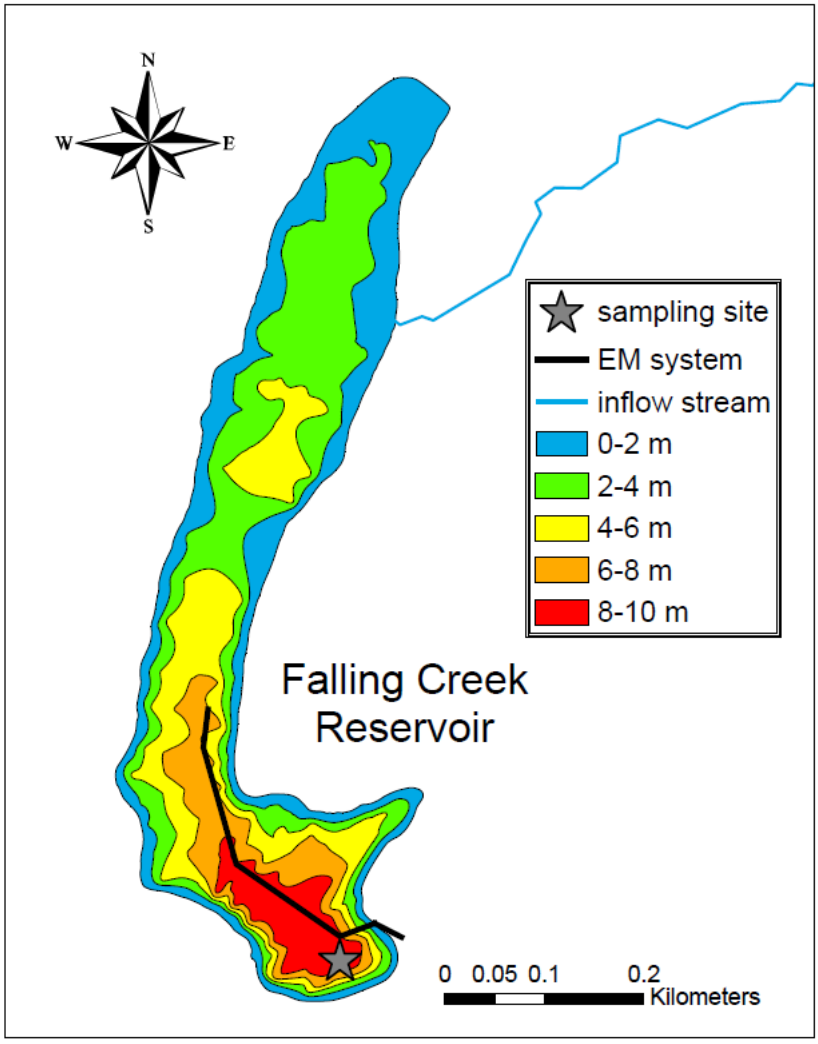

1173

1174

1175

1176

1177

1178

1179

1180

1181

1182

1183

1184 Figure 3

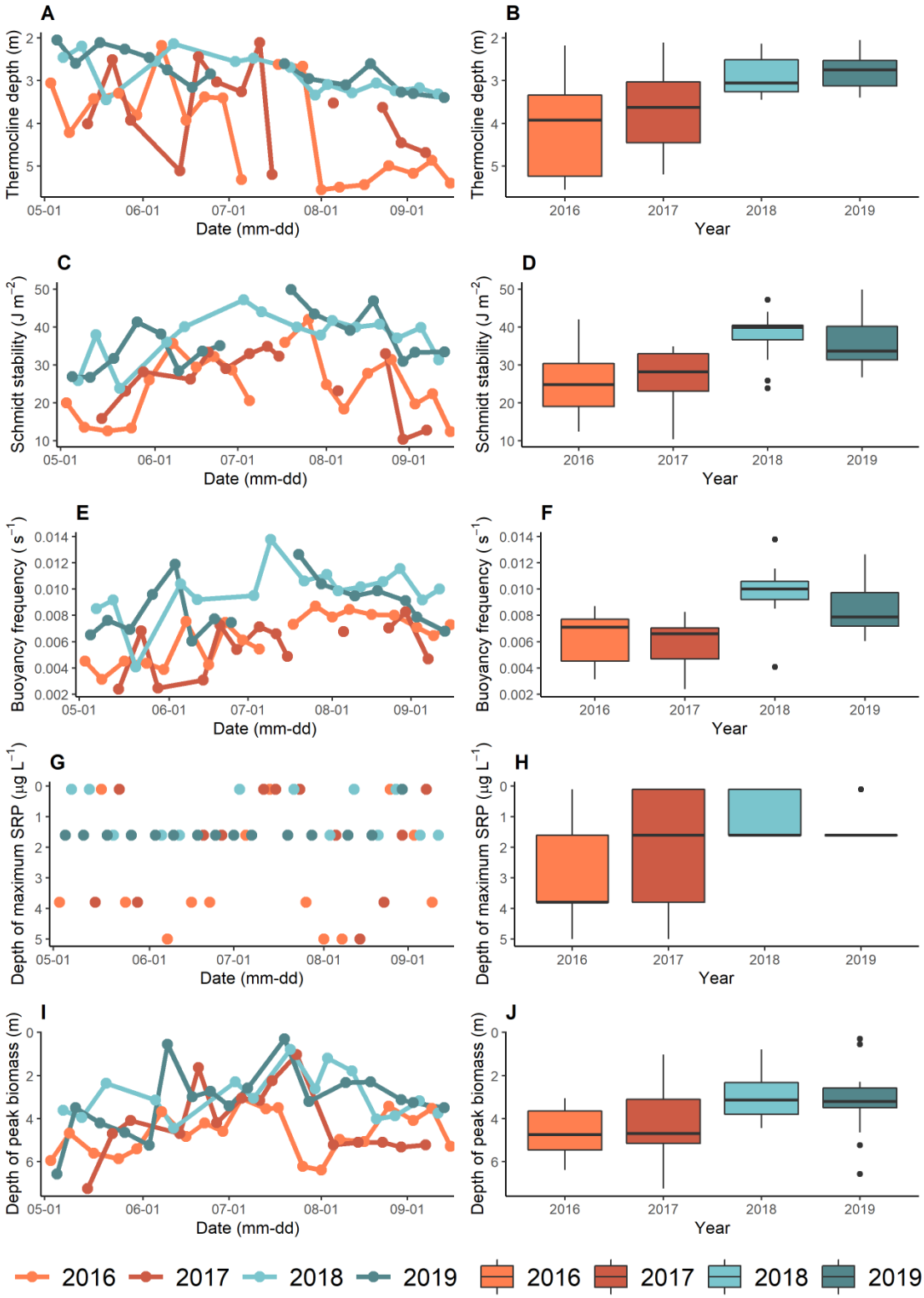

1185

1186

Figure 4

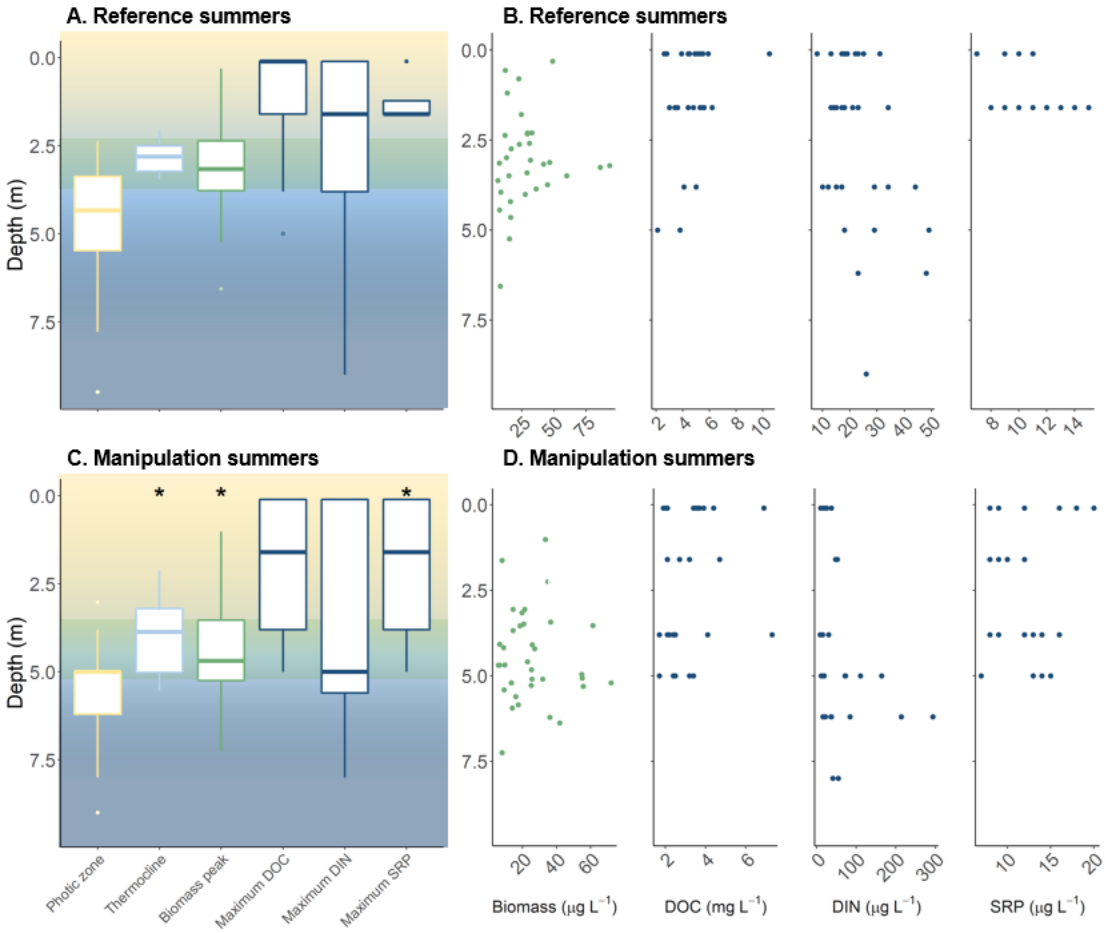
A. Reference summers
B. Reference summers
C. Manipulation summers
D. Manipulation summers
Depth (m)
0.0
2.5
5.0
7.5
*
Photic zone
Thermocline
Biomass peak
Maximum DOC
Maximum DIN
Maximum SRP
Biomass (μg L⁻¹)
DOC (mg L⁻¹)
DIN (μg L⁻¹)
SRP (μg L⁻¹)

Figure 5

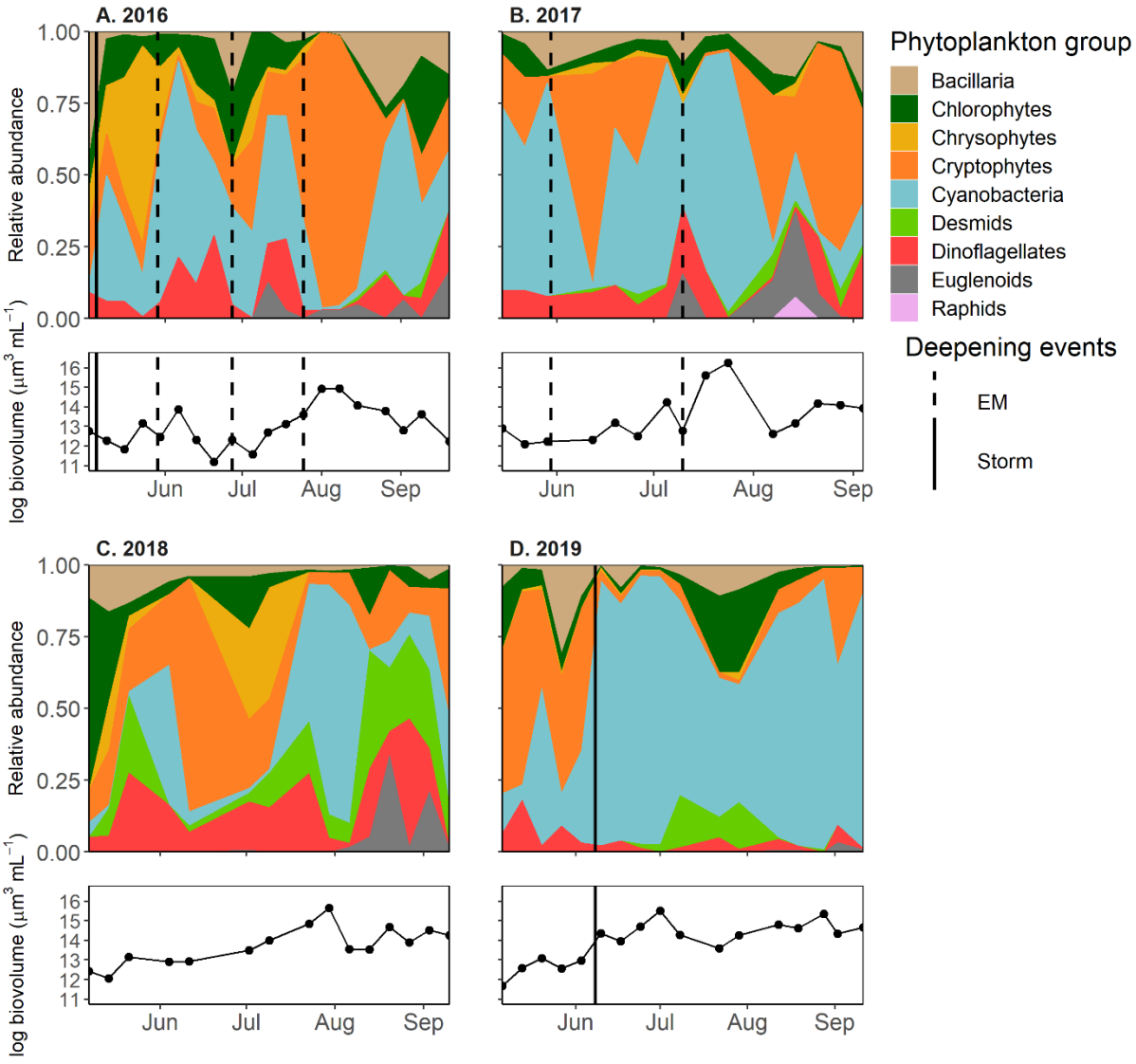
A. 2016
B. 2017
C. 2018
D. 2019
Relative abundance
log biovolume (µm³ mL⁻¹)
Jun
Jul
Aug
Sep
Phytoplankton group
Bacillaria
Chlorophytes
Chrysophytes
Cryptophytes
Cyanobacteria
Desmids
Dinoflagellates
Euglenoids
Raphids
Deepening events
EM
Storm

1204 Figure 6

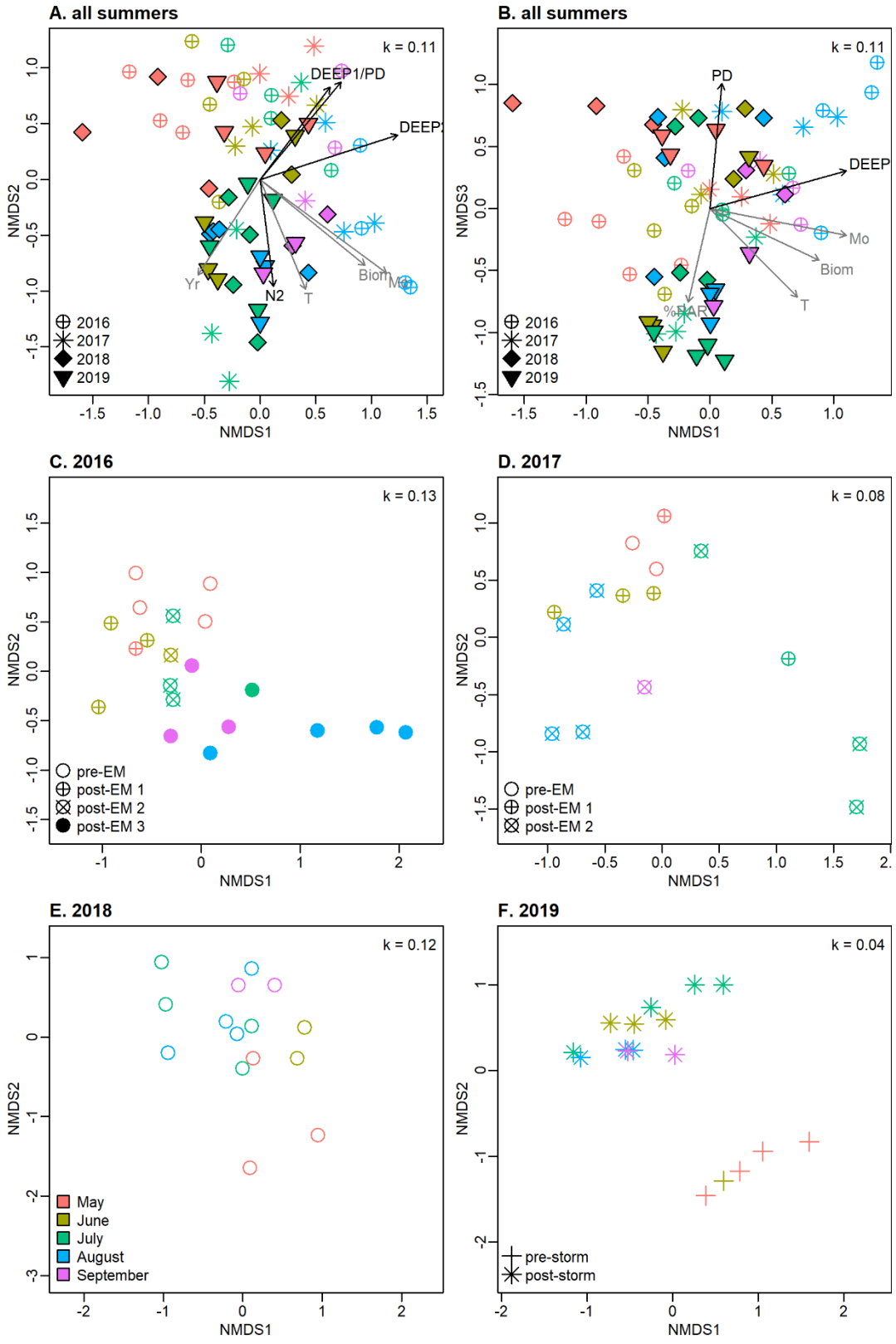

1205

1206 Figure 7

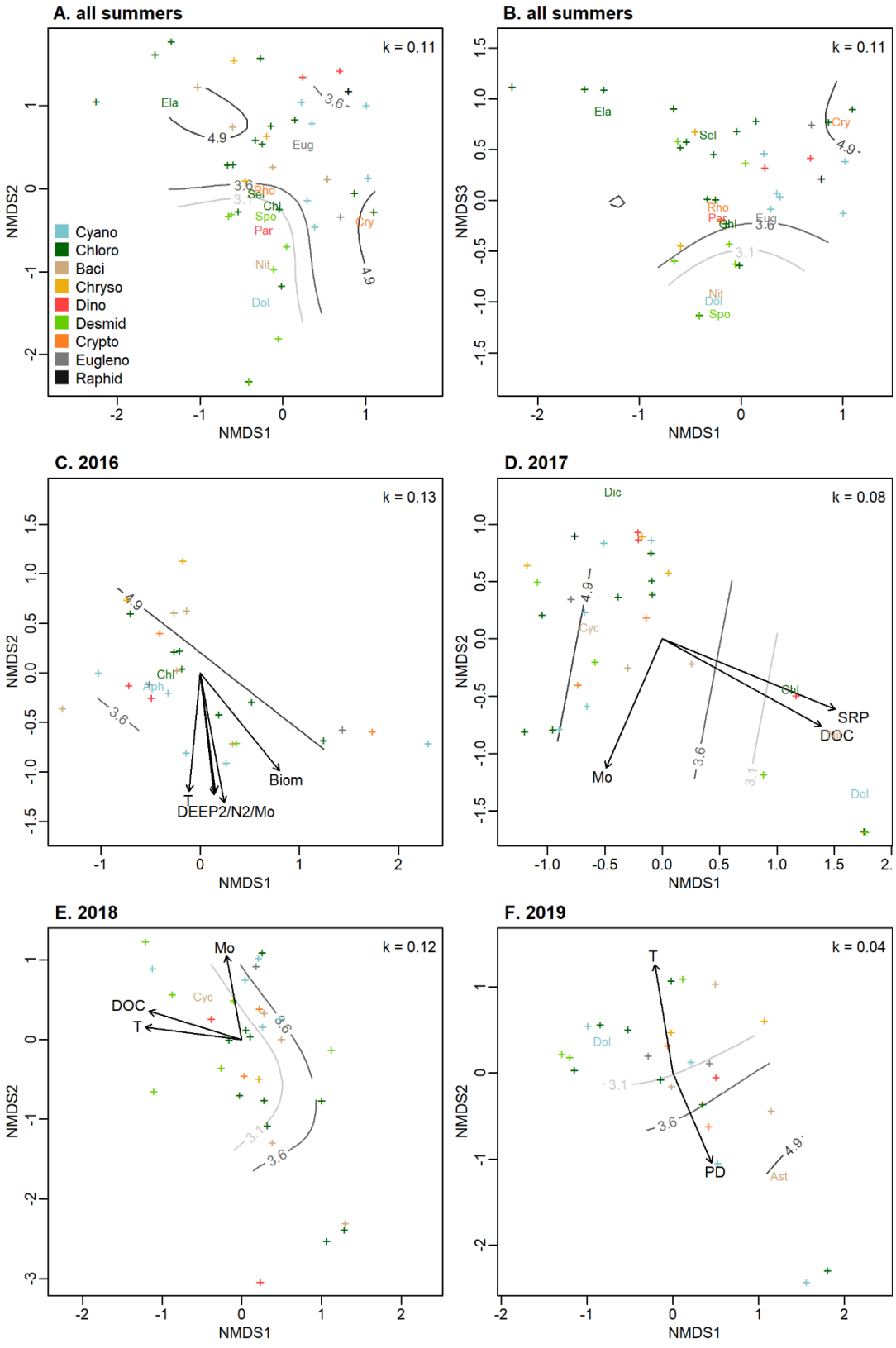

1207